THE UNIVERSITY OF CALGARY

KINETICS OF SOLVENT EXCHANGE ON SOME COPPER AND NICKEL COMPLEXES IN ACETONITRILE

BY

JOHN H. MACHIN

A THESIS

SUBMITTED TO THE FACULTY OF GRADUATE STUDIES

IN PARTIAL FULFILLMENT OF THE REQUIREMENTS FOR THE

DEGREE OF MASTER OF SCIENCE

DEPARTMENT OF CHEMISTRY

CALGARY, ALBERTA

SEPTEMBER, 1984

THE UNIVERSITY OF CALGARY

FACULTY OF GRADUATE STUDIES

The undersigned certify that they have read, and recommend to the Faculty of Graduate Studies for acceptance, a thesis entitled "Kinetics of Solvent Exchange on Some Copper and Nickel Complexes in Acetonitrile" submitted by John H. Machin in partial fulfillment of the requirements for the degree of Master of Science.

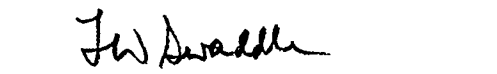

Supervisor, Dr. T.W. Swaddle
Department of Chemistry

Dr. H.A. Buckmaster
Department of Physics

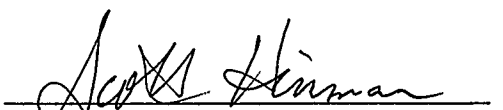

Dr. A.S. Hinman
Department of Chemistry

Dr. T.S. Sorenson
Department of Chemistry

DATE: September 26, 1984

ABSTRACT

An attempt was made to study the exchange of acetonitrile on some paramagnetic copper(II) and nickel(III) complexes using the broadened ^{14}N NMR signal of CH_3CN.

The study of $[Cu(tren)CH_3CN](ClO_4)_2$ and $[Cu(Me_6tren)CH_3CN](ClO_4)_2$ in CH_3CN indicates that formation of an ion-pair complex interferes with the solvent exchange. The equilibrium constant for ion-pair formation for the $[Cu(tren)CH_3CN]^{2+}$ complex is estimated to be $K_c(298)$ = 218 kg mol^{-1} and the enthalpy ΔH_c = 20 kJ mol^{-1}. The parameters for solvent exchange on $[Cu(tren)CH_3CN]^{2+}$ are found to be: ΔH^* = 39 kJ mol^{-1}, and $k_{ex}(298) = 1.33 \times 10^6$ s^{-1}. The observed rate of exchange for $[Cu(Me_6tren)CH_3CN]^{2+}$ was found to be at least 15 times slower than for the Cu(II)-tren complex. An estimated volume of activation, ΔV^*, for CH_3CN exchange on $[Cu(tren)CH_3CN]^{2+}$ of -2 cm^3 mol^{-1} was obtained, but this value is uncertain as there is a large volume change observed for the ion-pair formation, $\Delta V_c \simeq 30$ cm^3 mol^{-1}. These findings suggest that the exchange mechanism on the five-coordinate copper system is an associative one.

The complex $[Ni(cyclam)(CH_3CN)_2]X_3$ (X = ClO_4, CF_3SO_3) was not sufficiently stable in dilute solution in acetonitrile. The ^{14}N linebroadening observed was due to CH_3CN exchange on the high spin complex $[Ni(cyclam)(CH_3CN)_2]^{2+}$ which is in equilibrium with low spin $[Ni(cyclam)]^{2+}$. The equilibrium constant K_{eq} at 298 K is found to be 1.7 with ΔH = 20 kJ mol^{-1}, and the exchange parameters on the high spin complex are: ΔH^* = 32.1 ± 0.4 kJ mol^{-1}, ΔS^* = 76.2 ± 0.4 J K^{-1} mol^{-1}, and $k_{ex}(298) = 1.58 \times 10^6$ s^{-1}. These values suggest that the CH_3CN exchange on the Ni(II)-cyclam high spin complex follows a dissociative mechanism.

ACKNOWLEDGEMENTS

I would like to sincerely thank Dr. T.W. Swaddle for his assistance and patience during the course of this research.

I would also like to express my gratitude to Mr. D. Malinsky and Mr. T. Mani for their help in constructing the high pressure NMR probe, and to the many people of the Department whose friendship and support were invaluable to me.

Special thanks are given to Miss Anne Baird for her patience and care in typing this manuscript, to Dr. M. Sisley and Dr. N. Smith for their diligence in proofreading.

Financial support for this work from the Province of Alberta, in the form of a Graduate Scholarship, and from the University of Calgary is gratefully acknowledged.

TO MY PARENTS

WITH LOVE AND GRATITUDE

FOR THEIR SUPPORT AND ENCOURAGEMENT

TABLE OF CONTENTS

LIST OF TABLES

LIST OF FIGURES

Chapter 1 Introduction, Literature Survey, and Experimental Objectives

1.1 Introduction

The use of nuclear magnetic resonance for observing chemical exchange reactions was first proposed in 1953[1] and was first used in 1956.[2] It has since become an important method for observing the exchange of nuclei between magnetically (and chemically) different environments. The studies take place under equilibrium conditions and the use of variable temperature apparatus allows studies of exchanges on the order of 10^{-3} - 10^{6} s^{-1}.[3] Examples of some well-known processes that have been studied are the exchange of protons between axial and equatorial positions in cyclohexane,[4] and the rotation of methyl groups about the C-N bond of N,N-dimethylformamide.[5]

Kinetic studies of chemical reactions under high pressure conditions have been discussed by a number of workers[6-10] and have been shown to be a good method for gaining some insight into the reaction mechanism. The design and development of high pressure NMR equipment has been extensively reviewed by Jonas.[11-14] The early work was concerned with studies of the dynamic structure of simple liquids at high pressure, and the later work has involved more complicated exchange reactions.[15]

1.2 Literature Survey

The general approach to studying exchange reactions using NMR is to modify the Bloch equations to account for the effect of the exchange process. The expression developed by Swift and Connick[16,17] depends on the nuclear relaxation at one site being faster than at the other site, and on one site being in higher concentration than the other. A dilute

solution of a paramagnetic ion fulfills these conditions. A variable temperature study of such a solution gives NMR lines that are wider than those of the pure solvent. Application of transition state theory to the information obtained from the Swift-Connick equation leads to the activation parameters, ΔH^* and ΔS^*, for the exchange reaction [1-1].

$$ML_n + L^o \rightleftharpoons [ML_nL^o] \rightleftharpoons ML_{n-1}L^o + L \qquad [1\text{-}1]$$

Similarly the application of high pressure can lead to the volume of activation, ΔV^*, for the reaction. The entropy of activation and the volume of activation are useful in determining the mechanism of the reaction according to the Langford-Gray classification,[18] that is, whether the mechanism of exchange is associative, A, dissociative, D, associative interchange, I_a, or dissociative interchange, I_d.

Examples of systems studied using the Swift-Connick expression are listed in Table [1-1], along with rate constants and activation parameters. Most of this material has been reviewed in the specialist periodicals[53] and by Lincoln.[3] The majority of the work has investigated the exchange of solvent on the solvates of the paramagnetic ions. Other studies have investigated the effect on solvent lability of one or more chelating ligands coordinating to the metal ions.[39,49] Early studies were done using the more readily observed nuclei such as ^1H and ^{13}C. However as the use of multinuclear NMR has increased, ^{14}N and ^{17}O studies have become more common as the linebroadening is much more pronounced for ligand nuclei closest to the paramagnetic centre. Also, for aqua exchange the use of ^{17}O NMR removes complications due to hydrogen exchange by the solvent.

TABLE [1-1]

Activation parameters for Solvent Exchange

System	Nucleus	ΔH^* kJ mol^{-1}	ΔS^* J K^{-1} mol^{-1}	ΔV^* [b] cm^3 mol^{-1}	k_{ex} [a] s^{-1}	Ref.
$Al(DMSO)_6^{3+}$/DMSO	^1H			15.6±1.4 (358)		19
$Al(DMF)_6^{3+}$/DMF	^1H			13.7±1.2 (354)		19
$Ga(DMSO)_6^{3+}$/DMSO	^1H			13.1±1.0 (335)		19
$Ga(DMF)_6^{3+}$/DMF	^1H			7.9±1.6 (314)		19
$VO(CH_3CN)_4^{2+}/CH_3CN$	^1H	29.5	-84		2.85×10^3	20
$Cr(en)_3^{3+}$/DMSO[c]	^1H	27.6±2.1	-92±8		$(1.2\pm0.2)\times10^3$	21
$Cr(en)_3^{3+}$/DMSO[d]	^1H	104.6±2.1	109±8		$(1.4\pm0.2)\times10^3$	21

TABLE [1-1] cont.

$Mn(H_2O)_6^{2+}/H_2O$	^{17}O	33.9	12.1		3.1×10^7	16
		36.8±4.2	21±12		$(5.9\pm0.6)\times10^6$ (273)	22
$Mn(CH_3CN)_6^{2+}/CH_3CN$	^{14}N	15	-63			23
		29.6±0.5	-8.9±2.0	-7.0	1.36×10^7	24
		30.33±12.6	-7.5±3.4		$(1.2\pm0.3)\times10^7$	25
	^{1}H	35.9	19.0		3.1×10^7	26
$Mn(Phen)(H_2O)_4^{2+}/H_2O$	^{17}O	37.7±8.4	25±29		$(13\pm2)\times10^6$ (273)	22
$Mn(Phen)_2(H_2O)_2^{2+}/H_2O$	^{17}O	37.7±8.4	33±38		$(31\pm3)\times10^6$ (273)	27
$Mn(NTA)(H_2O)_2/H_2O$	^{17}O	27.6	25		$(1.5\pm0.8)\times10^9$	27
$Mn(EDTA)(H_2O)^{2-}/H_2O$	^{17}O	32.2	29		4.4×10^8	27
$Fe(H_2O)_6^{2+}/H_2O$	^{17}O	32.2	-12.6		3.2×10^6	16
$Fe(CH_3CN)_6^{2+}/CH_3CN$	^{14}N	41.4±0.7	5.3±2.5	+3.0	6.6×10^5	24
	^{1}H	36.4	-14.9		4.3×10^5	26
$Fe(CH_3CN)_6^{3+}/CH_3CN$	^{1}H				< 40	28
$Fe(DMF)_6^{3+}/DMF$	^{1}H	52.3±6.3	-41.8±20.9		33	28
	1H	42.3±4.2	-69.0±12.6		61	29

TABLE [1-1] cont.

	^{1}H			-0.9±0.2		30
$Fe(DMSO)_6^{3+}/DMSO$	^{1}H			-3.1±0.3		30
$Fe(CH_3OH)_6^{3+}/CH_3OH$	^{1}H			6.4±0.2		30
$Fe(CH_3CH_2OH)_6^{3+}/CH_3CH_2OH$	^{1}H	25.9±6.3	-75.3±20.9		2.0×10^4	28
$Fe^{III}(TPP)^+/DMF$	^{1}H	39.3±1.7	15.9±2.9		5.4×10^6	29
$Fe^{III}(TPP)^+/CH_3OH$	^{1}H	47.3	37.7		3.0×10^6	29
$Co(H_2O)_6^{2+}/H_2O$	^{17}O	33.5	-17.2		1.13×10^6	16
$Co(CH_3CN)_6^{2+}/CH_3CN$	^{14}N	47.7±2.1	20.9±8.4		$(3.2\pm0.3)\times10^5$	31
	^{1}H	47.7±2.1	21.8±9.2		$(3.5\pm0.5)\times10^5$	31
	^{14}N	36.78	-17.6		2.7×10^5	32
	^{1}H	33.9	-31.4±8.4		1.4×10^5	33
	^{13}C	48.79±1.1	22.2±3.7	7.7±1.7	$(2.56\pm0.6)\times10^5$	34
	^{1}H			9.9±0.7 (260)		35
	^{14}N			+6.7		36
$Co(DMF)_6^{2+}/DMF$	^{1}H			6.7±0.3 (296)		35
$Co(CH_3OH)_6^{2+}/CH_3OH$	^{1}H			8.9±0.3 (279)		35
$Co(DMSO)_6/DMSO$	^{1}H	38.1±4.2	-10.0±12.6		$(3.40\pm0.4)\times10^5$	37

Table [1-1] cont.

$Co(tren)CH_3CN^{2+}/CH_3$	^{14}N				$\geq 2\times10^6$ (233)	38
$Co(Me_6tren)CH_3CN^{2+}/CH_3CN$	^{14}N				$\leq 0.1\times10^3$ (353)	39
$Co(trenol)(CH_3CN)_2^{2+}/CH_3CN$	^{14}N				$\geq 2\times10^6$ (223)	39
$Co(triol)(CH_3CN)_3^{2+}/CH_3CN$	^{14}N	40±2	-9.6±6.2		$(23\pm2)\times10^4$	39
$Co(cyclam)(CH_3CN)_2^{2+}/CH_3CN$	^{14}N				$\geq 8\times10^6$ (266)	39
$Co(Me_4cyclam)(CH_3CN)_2^{2+}/CH_3CN$		^{13}C			-9.6±0.5	40
$Ni(H_2O)_6^{2+}/H_2O$	^{17}O	48.5	2.5		2.7×10^4	16
		43.1±2.1	-21.8±8.4		$(4.4\pm0.2)\times10^4$	41
		64.3±0.9	37.0±2.8	7.1±0.2	$(3.37\pm0.09)\times10^4$	42
$Ni(CH_3CN)_6^{2+}/CH_3CN$	^{14}N	68.4±2.0	50±8.0		$(2.0\pm0.3)\times10^3$	43
	^{1}H	59.6±8.8	23±16.7		$(3.6\pm0.6)\times10^3$	43
	^{14}N	39.5	-32.6		1.45×10^4	32
	^{14}N	60.8±1.1	25.8±2.8	7.3	3.1×10^3	36
	^{1}H	51.8	-4.0		3.15×10^3	26
	^{1}H	45.6±2.1	-36.8		3.9×10^3	33
	^{1}H	64.3±0.9	37.0±2.8	9.6±0.4	(2.84±0.05)	44
	^{1}H			9.6±0.3 (294)		35

Table [1-1] cont.

$Ni(DMSO)_6^{2+}/DMSO$	^1H	56.1±2.5	21.8±6.3		1.14×10^4	37
$Ni(CH_3CH_2OH)_6^{2+}/CH_3CH_2OH$	^1H	45.2±6.3	-16.7±20.9		1.1×10^4	28
$Ni(NH_3)_6^{2+}/NH_3(aq)$	^{14}N	57.3±0.3	40.2±0.8	5.9	$(6.96\pm0.05)\times10^4$	45
$Ni(triol)(CH_3CN)_3^{2+}/CH_3CN$	^{14}N	66.5±3.4	36.4±10.5		$(1.0\pm0.2)\times10^3$	46
$Ni(triam)(CH_3CN)_3^{2+}/CH_3CN$	^{14}N	38.9±4.2	-3.8±14.6		$(555\pm60)\times10^3$	46
$Ni(diamol)(CH_3CN)_3^{2+}/CH_3CN$	^{14}N	50.2±4.6	22.6±14.6		$(180\pm30)\times10^3$	46
$Ni(trenol)(CH_3CN)_2^{2+}/CH_3CN$	^{14}N	50.2±5.0	11.7±16.7		$(40\pm6)\times10^3$	46
$Ni(Me_6tren)(CH_3CN)_2^{2+}/CH_3CN$	^{14}N				$\leq 0.1\times10^3$ (353)	38
$Ni(tren)(CH_3CN)_2^{2+}/CH_3CN$[e]	^{14}N	45.2±6.3	5.9±20.9		$(165\pm35)\times10^3$	38
$Ni(tren)(CH_3CN)_2^{2+}/CH_3CN$[f]					$\geq 2\times10^6$ (233)	38
$Ni(tren)(H_2O)_2^{2+}/H_2O$[g]	^{17}O	33.5±4.2			8.2×10^5	47
$Ni(tren)(H_2O)_2^{2+}/H_2O$[h]		33.5±6.3			$\sim 9\times10^6$	47
$Ni(tren)(H_2O)_2^{2+}/H_2O$[i]					1.5×10^6	47
$Ni(DMF)_6^{2+}/DMF$	^1H			9.1±0.3 (297)		35
$Ni(CH_3OH)_6^{2+}/CH_3OH$	^1H			12.4±0.6 (307)		35
				10.9±0.6		48
$Ni(Me_4cyclam)(CH_3CN)^{2+}/CH_3CN$	^{13}C			2.3±1.3		40

Table [1-1] cont.

$Cu(H_2O)_6^{2+}/H_2O$	^{17}O	46.0	-16		1.0×10^4	16
$Cu(CH_3CN)_6^{2+}/CH_3CN$	^{1}H	20			$\gg 3.7\times10^8$	26
					$\gg 3.1\times10^7$ (228)	26
	^{14}N				$\geq 1.6\times10^7$ (228)	49
$Cu(CH_3OH)_6^{2+}/CH_3OH$	^{17}O	25.1	-10.9		7.4×10^7	51
$Cu(trenol)CH_3CN^{2+}/CH_3CN$	^{14}N	26±8	-34±32		$(8.0\pm2)\times10^4$ (228)	49
$Cu(Me_6tren)CH_3CN^{2+}/CH_3CN$	^{14}N				$< 10^2$ (228)	
$Cu(tren)CH_3CN^{2+}/CH_3CN$	^{14}N	45±4	26±16		$(5.1\pm0.7)\times10^3$	49
$Cu(tren)H_2O^{2+}/H_2O$	^{17}O	10.4±0.3			2.5×10^5	47
$TaBr_5.Me_2O/Me_2O$	^{1}H			30.5±2.0		50
$TaBr_5.Me_2S/Me_2S$	^{1}H			-12.6±1.0		50

a) 298 K unless otherwise indicated

b) numbers in parentheses indicate temperature

c) 2nd coordination sphere exchange

d) partially dissociated $Cr(en)_3^{3+}$

Table [1-1]

e) } two exchange sites $[Ni(tren)(CH_3CN)_2]^{2+}$,
f) } axial and equatorial

g) at 25°C

h) 25°C value extrapolated from values at -10°C

i) at -10°C

From Table [1-1] it can be seen that the rate constant, k_{ex}, for exchange is reproducible, but the activation parameters obtained by different workers can vary considerably. This problem has been discussed previously.[53] The discrepancy arises from the simplifications introduced by various workers to solve the nonlinear Swift-Connick expression. A further problem is that ΔS^* and ΔH^* are highly correlated and vary linearly with one another.[54] ΔH^* is determined from the slope of a line over a relatively short temperature range that is far from the origin. Therefore a small error in slope (= $\Delta H^*/R$) can lead to a large error in the intercept (= $\Delta S^*/R$). In contrast, the volume of activation can be more accurately determined, as it is derived from the pressure dependence of the rate constant.

The significance of the activation parameters, ΔS^* and ΔV^*, has recently been reviewed.[55] If the exchange, equation [1-1], goes through a dissociative process, D or I_d, then the parameters ΔS^* and ΔV^* are expected to be positive. Similarly for an associative type exchange, A or I_a, the values are expected to be negative. Therefore the values of ΔS^* and ΔV^* can give some indication as to the type of exchange mechanism that takes place.

It can be noted, from Table [1-1], that as we move across the first row transition elements, the volume of activation for solvent exchange changes from a negative value to a positive one. This implies that there is a change in mechanism on going across the first row of elements. This trend, along with a trend towards more associative behaviour on going down a group of elements, has been discussed in more detail by Merbach.[55] Some explanations for these trends have been proposed:

1) decreasing ionic radii cause steric crowding at the transition state, such that dissociation becomes the more favorable mechanism.
2) for octahedral complexes the t_{2g} orbitals are nonbonding and the e_g orbitals are σ^* antibonding; as the t_{2g} orbitals are filled the approach of a seventh molecule for an associative process becomes less electrostatically favorable.
3) however the V^{2+} ion is less associative than Mn^{2+}; this is explained by considering the occupancy of the e_g (σ^* antibonding) orbitals. The antibonding nature of these orbitals means that their filling introduces more dissociative character to the exchange.

1.3 Objectives

The objective of this work was to study the solvent exchange on some complexes of copper(II) and nickel(III) in acetonitrile. These complexes are d^9 and low-spin d^7 respectively, and therefore have the unpaired electron necessary to form a paramagnetic centre.

The copper complexes studied are $[Cu(tren)CH_3CN](ClO_4)_2$, where tren = tris(2-aminoethyl)amine, and $[Cu(Me_6tren)CH_3CN](ClO_4)_2$, Me_6tren = tris(N,N',N"-dimethyl-2-aminoethyl)amine. The X-ray structure studies of the copper-tren complex with bromine and thiocyanate indicate that in the solid state it has a trigonal bipyramidal configuration.[56,57] The inability of $[Cu(tren)H_2O]^{2+}$ to form more than a 1:1 compound with $NH_3(aq)$[47] and the similarity of the electronic spectra for both the Cu-tren and -Me_6tren complexes, to those of trigonal bipyramidal five coordinate compounds[58-60], indicate that this configuration is retained in solution (Figure [1-1]).

FIGURE [1-1]

Structure of $[CuLCH_3CN]^{2+}$

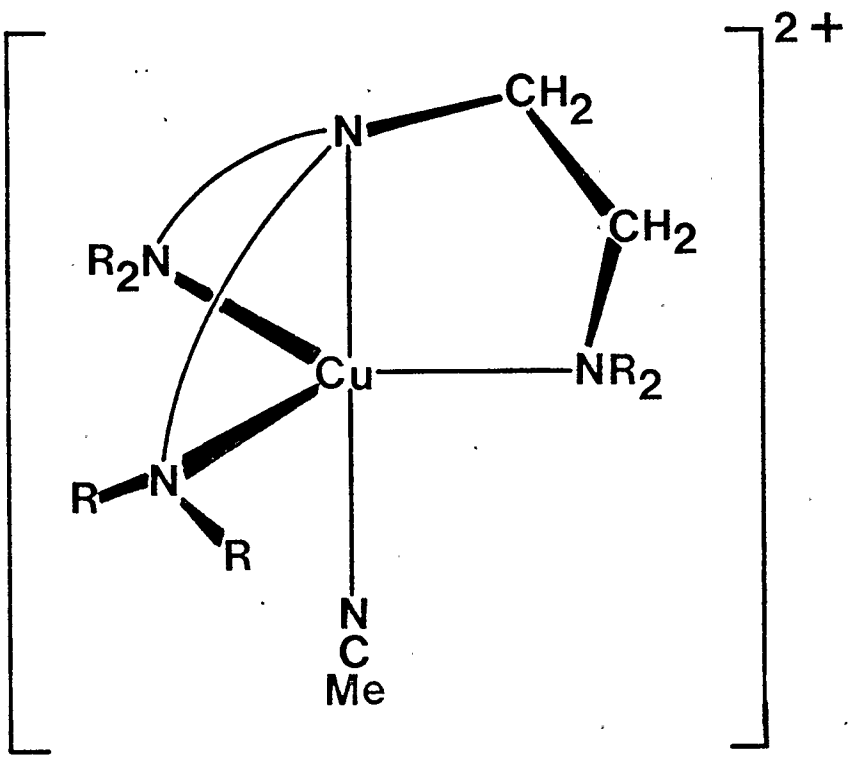

R = H : L = tren

R = Me : L = Me_6tren

Previous studies suggest the exchange on $[Cu(tren)sol]^{2+}$, sol = solvent, follows an associative mechanism at a rate 10^3 times slower than for the hexasolvated copper(II) ion.[49,61,62] This is in contrast to what is observed for the analogous cobalt(II) and nickel(II) systems, which show an increased solvent lability upon coordination of the tren ligand.[62] The solvent exchange on $[Cu(Me_6tren)sol]^{2+}$ is even slower and experimental evidence suggests that a dissociative type mechanism takes place.[63,64]

The nickel complexes studied were $[Ni(cyclam)(CH_3CN)_2]X_2$ and $[Ni(cyclam)(CH_3CN)_2]X_3$, (cyclam = 1,4,8,11-tetraazacyclotetradecane) where X = ClO_4 and CF_3SO_3. The structure in solution is octahedral with the cyclam ligand occupying the equatorial positions and the solvent molecules the axial positions[65] (Figure [1-2]). The chemistry of macrocyclic compounds has been reviewed extensively,[66,67] with those of nickel(III) having been reviewed separately.[65,68] Studies of complex formation suggest that a dissociative mechanism takes place in the substitution of solvent by a coordinating anion.[65,69] Aqua exchange studies on high-spin Ni(II) cyclam also indicate a dissociative mechanism.[70] Acetonitrile exchange on the N-methylated complex, $[Ni(Me_4cyclam)CH_3CN]^{3+}$($Me_4$cyclam = 1,4,8,11,-tetramethyl-1,4,8,11-tetraazacyclotetradecane) follows an associative mechanism; this complex, however, is five-coordinate.[40,71,72]

FIGURE [1-2]

Structure of $[Ni(cyclam)(CH_3CN)_2]^{3+}$

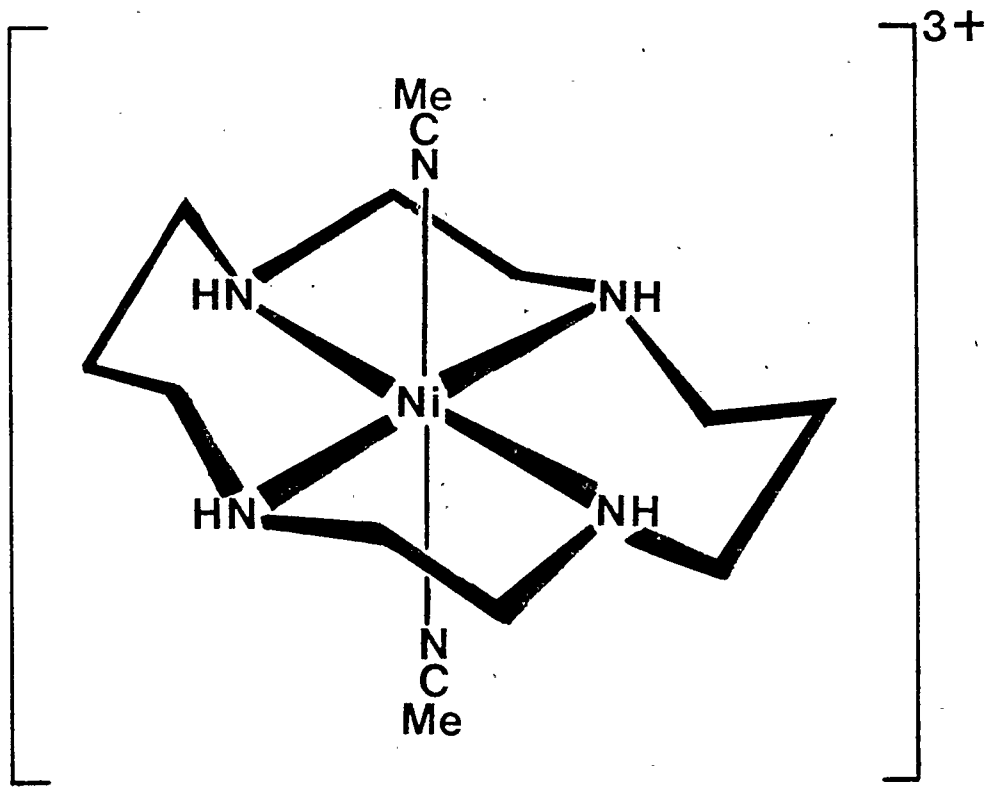
3+
Me
C
N
HN
NH
Ni
HN
NH
N
C
Me

Chapter 2 NMR Line Broadening Mechanisms

2.1 Variable Temperature

The transverse relaxation time, T_2, for ^{14}N NMR in pure acetonitrile has been found to equal the longitudinal relaxation time, T_1.[73-75] The temperature dependence of the relaxation can be described by the Arrhenius expression, equation [2-1]:

$$T_1 = T_2 = (\pi \nu_{1/2})^{-1} = A_{T_1} \exp (E_{T_1}/RT) \qquad [2\text{-}1]$$

where $\nu_{1/2}$ is the full width of the NMR resonance line at half height. For a solution containing paramagnetic ions the full Swift-Connick equation[16,17] [2-2]

$$(P_m T_{2p})^{-1} = \tau_m^{-1} \frac{T_{2m}^{-2} + (T_{2m}\tau_m)^{-1} + \Delta\omega_m^2}{(T_{2m}^{-1} + \tau_m^{-1})^2 + \Delta\omega_m^2} + \frac{1}{T_{2os}} \qquad [2\text{-}2]$$

describes the contribution to the linewidth due to paramagnetic relaxation and exchange of solvent between the bulk solvent and the coordination site on the ion.

The term T_{2p}^{-1} is the difference in reciprocal transverse relaxation times between the solution containing the paramagnetic ions and the pure solvent, equation [2-3].

$$T_{2p}^{-1} = T_{2obs}^{-1} - T_{2solvent}^{-1} = \pi \nu_{1/2\ obs} - \pi \nu_{1/2\ solvent} = \pi \Delta\nu_{1/2} \qquad [2\text{-}3]$$

The mole fraction, P_m, is included to remove the dependence of the increase in linewidth on the concentration. The term T_{2m}^{-1} is the relaxation term for nuclei of solvent coordinated to the paramagnetic centre. The T_{2os}^{-1} term is the relaxation of nuclei of solvent located in the second solvation sphere of the paramagnetic ion. Both of the relaxation terms, T_{2m}^{-1} and T_{2os}^{-1}, have a temperature dependence that can be expressed using the Arrhenius equation, equations [2-4] and [2-5].

$$T_{2m}^{-1} = A_m \exp(E_m/RT) \qquad [2\text{-}4]$$

$$T_{2os}^{-1} = A_{os} \exp(E_{os}/RT) \qquad [2\text{-}5]$$

The time constant, τ_m, for the exchange is the reciprocal of the rate constant, k_{ex}, and from transition state theory has a temperature dependence given by the Eyring equation [2-6].

$$\tau_m^{-1} = k_{ex} = \frac{\kappa T}{h} \exp\left[\frac{\Delta S^*}{R} - \frac{\Delta H^*}{RT}\right] \qquad [2\text{-}6]$$

The temperature dependence of the resonance frequency shift for the solutions from the frequency of pure solvent, $\Delta\omega_m$, can be described by equation [2-7], which is based on the Curie law.[24]

$$\Delta\omega_m/\omega_o = 2\pi(A/h)\ \mu_{eff}\ \mu_B[S(S+1)]^{1/2}/3kT\gamma_N \qquad [2\text{-}7]$$

A plot of $(P_m T_{2p})^{-1}$ versus $1/T$, see equation [2-2], gives a curve (Figure [2-1]) having four regions[44] in which some limiting equations can be used.

FIGURE [2-1]

Temperature dependence of paramagnetic relaxation

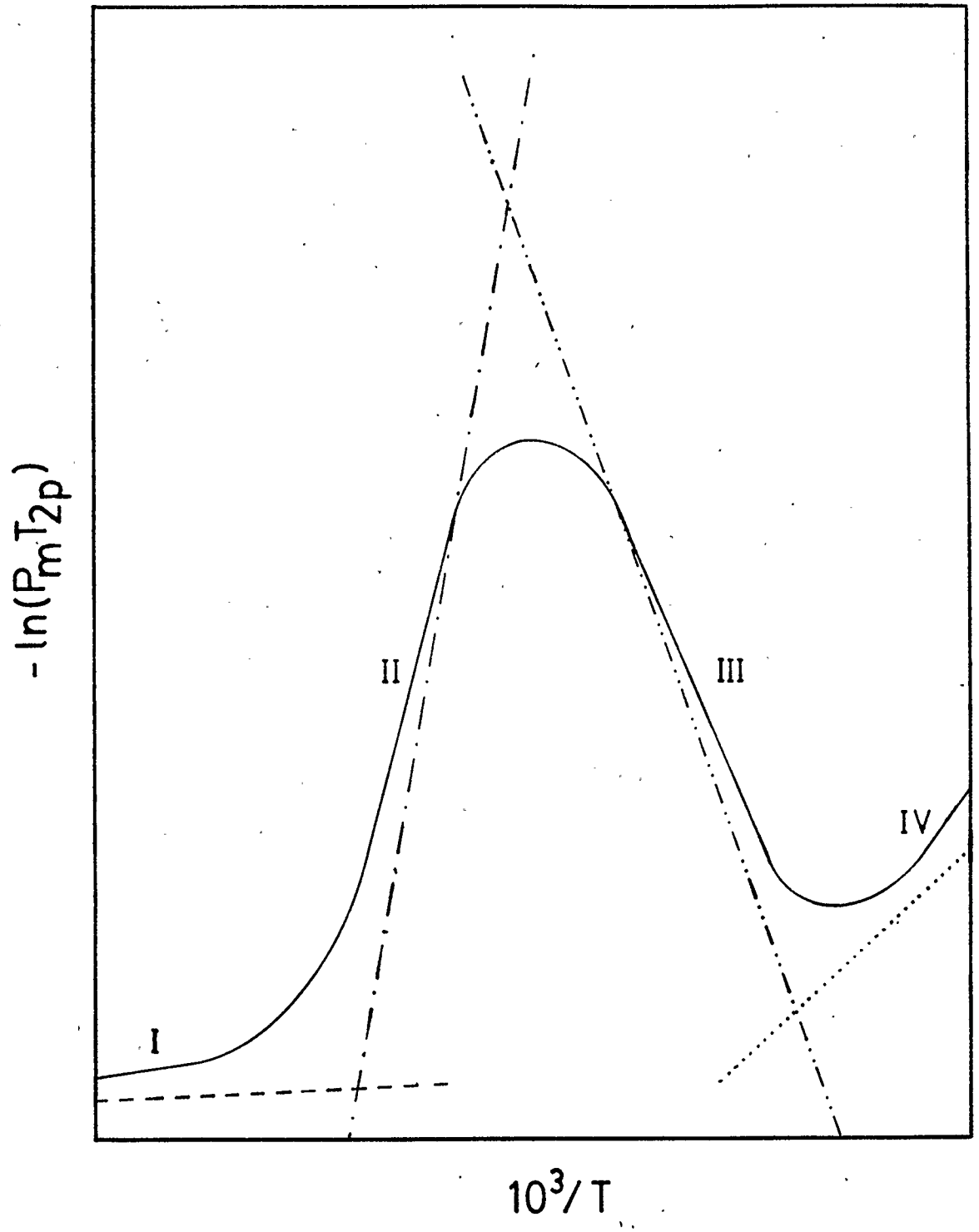
- ln(P_m T_2p)
II
III
IV
I
10^3/T

In region I, at high temperatures, the chemical exchange is faster than the NMR timescale. As a result the observed relaxation is due to the solvent coordinated to the paramagnetic ion, equation [2-8].

$$(P_m T_{2p})^{-1} = T_{2m}^{-1} \qquad [2\text{-}8]$$

As the temperature is lowered, the exchange rate slows down to the NMR timescale and a single peak that is exchange broadened is observed. The relaxation in this region, region II, is dominated by the fast chemical exchange, equation [2-9].

$$(P_m T_{2p})^{-1} = \Delta\omega_m^{\,2}\, \tau_m \qquad [2\text{-}9]$$

Further lowering of the temperature leads to splitting of the peak into resonance peaks for the bulk solvent and the solvent coordinated to the paramagnetic ion, region III. However ^{14}N has a spin of I=1, therefore the peaks are broadened by the electric quadrupole moment and this splitting is observed as an increased broadening of the single peak. The relaxation of the bulk solvent will be affected by chemical exchange as given by equation [2-10].

$$(P_m T_{2p})^{-1} = \tau_m^{-1} \qquad [2\text{-}10]$$

In region IV, the temperature has been lowered to the point where the chemical exchange is slower than the NMR timescale. The relaxation becomes dependent on the solvent molecules in the second solvation sphere about the paramagnetic ion, equation [2-11].

$$(P_m T_{2p})^{-1} = T_{2os}^{-1} \qquad [2\text{-}11]$$

The dashed lines of Figure [2-1] show the temperature dependence of the limiting expressions [2-8] - [2-11]. Therefore, for paramagnetic solutions having limiting relaxation behaviour as illustrated in regions II and III, the equations [2-9] and [2-10] can be used in conjunction with the Eyring equation [2-6] to obtain approximate values of the activation parameters, ΔH^* and ΔS^*. The use of the full Swift-Connick expression [2-2], instead of these limiting expressions, should give more precise values of the activation parameters.

2.2 Variable Pressure

For pure acetonitrile the pressure dependence of T_1 (= T_2 = $1/\pi\nu_{1/2}$) is given by equation [2-12],[36]

$$(\partial \ln T_1/\partial P)_T = -\Delta V_\perp^*/RT \qquad [2\text{-}12]$$

where the term $\Delta V_\perp^*$ is the volume of activation for diffusion by rotation about an axis perpendicular to the C_{3v} axis of the molecule.

For a chemical reaction, the reaction rate is given by the Eyring equation [2-13].

$$k = \kappa T/h \exp(-\Delta G^*/RT)$$

or

$$\ln k = \ln(\kappa T/h) - \Delta G^*/RT \qquad [2\text{-}13]$$

Differentiation with respect to the pressure, at constant T, leads to equation [2-14].

$$(\partial \ln k/\partial P)_T = -\Delta V^*/RT \qquad [2\text{-}14]$$

This equation becomes equation [2-15] if ΔV^* is independent of the pressure.

$$\ln(k/k_o) = -(\Delta V^*/RT)P \qquad [2\text{-}15]$$

Where ΔV^* is not independent of P, another parameter, the compressibility coefficient of activation, $\Delta\beta^*$, can be introduced.[6,7,55] This parameter is defined by

$$\Delta\beta^* = -(\partial\Delta V^*/\partial P)_T \qquad [2\text{-}16]$$

Thus, for some temperature where the relaxation parameter, $(P_m T_{2p})^{-1}$, is directly related to the exchange rate, τ_m^{-1} (equations [2-9], [2-10]), the pressure dependence of the rate constant can be observed and the activation volume, ΔV^*, can be found. For simplicity it is important to choose a temperature at which only one relaxation process is significant, i.e. the middle of the temperature range of either region II or region III. At temperatures towards the ends of these regions the other processes start making significant contributions to $(P_m T_{2p})^{-1}$.

2.3 Correlation of activation parameters and solvent exchange mechanism

The Langford-Gray classification system[18] can be used to describe the ligand exchange reaction [2-17].

$$ML_nX + Y \rightleftharpoons [ML_n,X,Y] \rightleftharpoons ML_nY + X \qquad [2\text{-}17]$$

If an intermediate with either increased or decreased coordination number can be detected, then the mechanism is classified as associative, A, or dissociative, D, respectively. However, if no intermediate can be detected the exchange is classified as an interchange, I, and can either be associative, I_a, or dissociative, I_d.

One would expect that for an I_a mechanism, where bond formation occurs on forming the intermediate, that the value of ΔS^* would be negative. Conversely for an I_d mechanism ΔS^* should be positive. However the ΔS^* values have been shown to be unreliable in magnitude and in sign[44] as a result of oversimplification and compensation errors.[54]

The activation parameter ΔV^* should also be dependent on the reaction mechanism since the bond formation, in an I_a mechanism, should result in a smaller volume, application of pressure causing the rate of exchange to accelerate. Similarly for an I_d mechanism the bond stretching gives rise to an increased volume and therefore application of pressure decreases the rate of exchange. When the species exchanging in equation [2-17] are ionic there is an electrostrictive effect on the solvent, due to the dipoles formed in the transition state.[76] As a result the volume of activation observed will contain an intrinsic contribution from the changing internuclear distances and a contribution due to the electrostrictive effect, equation [2-18].

$$\Delta V^{*}_{obs} = \Delta V^{*}_{int} + \Delta V^{*}_{elec} \qquad [2\text{-}18]$$

Under some conditions ΔV^{*}_{elec} can become dominant and ΔV^{*}_{obs} no longer depends on the exchange mechanism. However, for solvent exchange, X = Y = the neutral solvent, and no significant dipoles are generated **en route** to the transition state so the observed volume of activation is given by equation [2-19].

$$\Delta V^{*}_{obs} \simeq \Delta V^{*}_{int} \qquad [2\text{-}19]$$

Therefore ΔV^{*}_{obs} should give some indication of the type of exchange mechanism that takes place.

Chapter 3 Experimental Methods

3.1 General

Fisher ACS grade acetonitrile was distilled three to four times from molecular sieves and phosphorus pentoxide. The dried solvent was then degassed by three to four freeze-pump-thaw cycles on a vacuum line. Any further work with the solvent, such as preparation of solutions or synthesis of complexes, was done under a dry nitrogen atmosphere in a glovebox.

The NMR experiments were done on a Bruker WH-90 (90 MHz ^{1}H, 6.479 MHz ^{14}N) Fourier transform spectrometer. The spectrometer was run in the quadrature detection mode with a sweep width of 20,000 Hz and a pulse width of 35 μs. A typical line width measurement involved the collection of 10,000 - 20,000 scans, with a delay time of 900 μs, of 2k data points, over a time span of one hour. Solutions used for the atmospheric pressure, variable temperature experiments were sealed into 5 mm NMR tubes which were held coaxially, by PTFE spacers, in 10 mm NMR tubes containing the lock compound. These solutions were thermostated using the Bruker temperature control apparatus. The temperature was measured, before and after each experiment, by means of a copper-constantan thermocouple immersed in silicone oil in a titanium tube that was placed within the r.f. coil of the spectrometer.

The high pressure NMR experiments were performed using a probe similar to the design of Merbach et al.[77] (Figure [3-1]). The pressure vessel was made from the titanium alloy IMI-680, and had a double helix cut into the outside surface for passage of a thermostating fluid. A brass jacket was shrunk-fit over the outside of the vessel to form the outer wall of the cooling jacket. The sealing plug at the bottom of the

FIGURE [3-1]

High pressure NMR probe

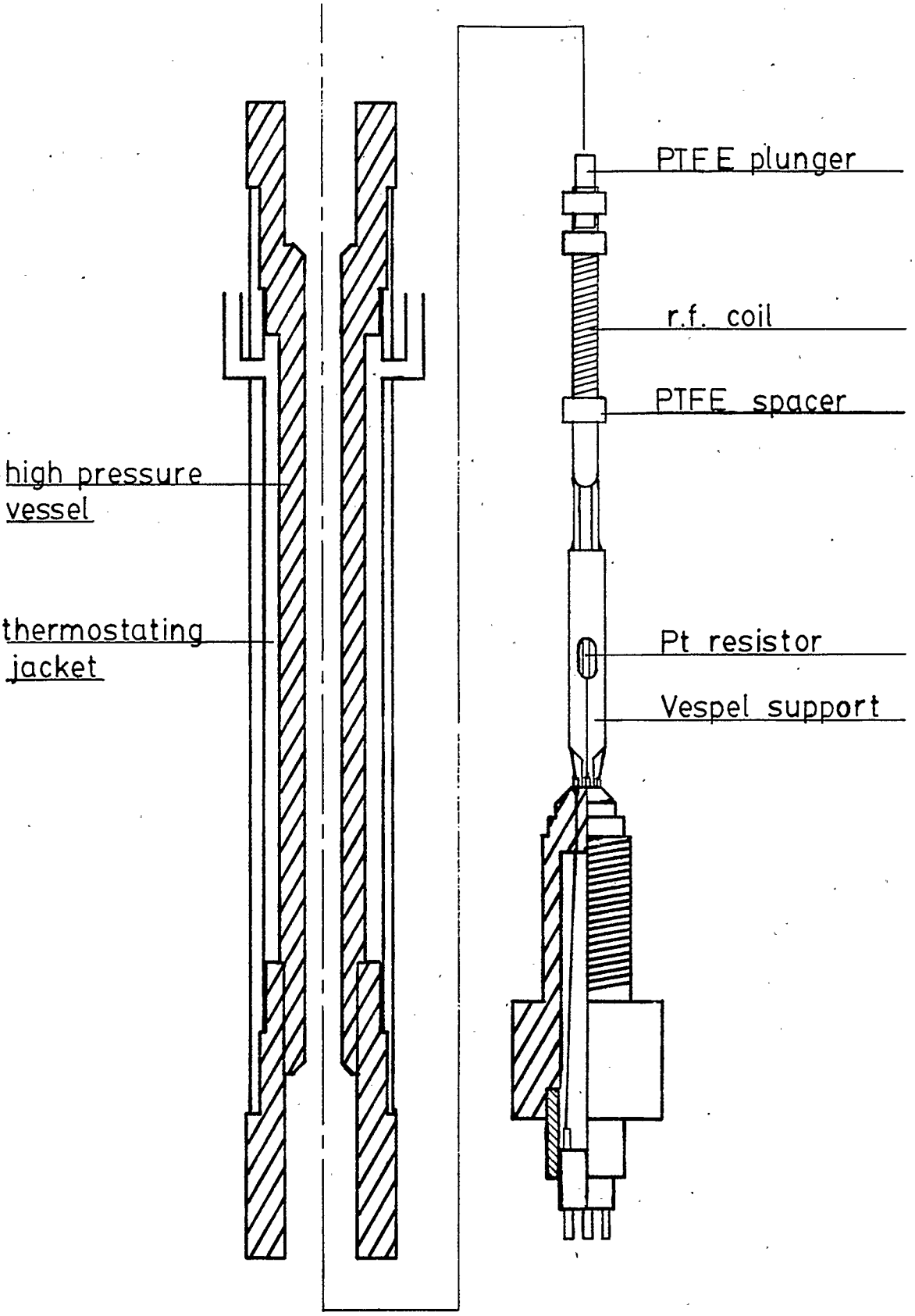
PTFE plunger
r.f. coil
PTFE spacer
high pressure vessel
thermostating jacket
Pt resistor
Vespel support

vessel was made up of a beryllium-copper alloy (Berylco 25) shaped into a Bridgman seal. Through this plug four wires were passed, electrically isolated with Vespel sleeves, to provide connections for the r.f. coil and thermistor. The sample was placed inside the glass tube on which the coil was wrapped and pressure was transmitted to the sample by a PTFE plunger in the open end. The sample tube was held coaxially in the bomb by teflon spacers and was held vertically by a Vespel support. The support was hollowed out below the sample to provide space for a platinum resistor, used for temperature measurement. This apparatus was pressurized with hexanes separated from an oil filled system with a PTFE separator. The pressures were produced with a small capacity screw press (Nova Swiss, range 0-4 kbar) and measured with a transducer (Autoclave Engineers, Model 6550-06-0-B; range 0-4 kbar) and digital readout (Autoclave Engineers, model DPS-0601; range 0-4 kbar). The platinum resistor was calibrated, in the magnetic field, against a copper-constantan thermocouple placed in the sample tube. The resistance was measured using a digital multimeter (Hewlett Packard 3468A) with either two or four lead wires. The dependence of the resistance on temperature (Table [3-1]) is shown in Figure [3-2]. When two lead wires were used for the measurement the temperature was given by equation [3-1a]. With the use of four lead wires the temperature was given by equation [3-1b], however for the pressure experiments on the nickel compound the circuit was rebuilt and recalibration gave equation [3-1c].

$$T(°C) = (2.92 \pm 0.04)R(\Omega) - (305.28 \pm 4.06) \qquad [3\text{-}1a]$$

$$T(°C) = (2.76 \pm 0.07)R(\Omega) - (280.15 \pm 7.99) \qquad [3\text{-}1b]$$

TABLE [3-1]

Temperature dependence of Pt resistor

Thermocouple (°C)	Resistance (Ω)
two lead wires, r = 0.9986	
31.9	115.390
30.4	114.811
24.4	112.760
21.5	111.726
20.9	111.485
16.6	109.970
15.4	109.479
14.9	109.531
12.2	108.457
10.1	107.989
8.6	107.091
5.9	106.576
5.2	105.839
3.3	105.340
2.6	105.503
0.2	104.056
-1.1	104.279
-3.4	103.502
four lead wires, r = 0.9975	
35.0	113.990
30.1	112.272
25.2	110.531
18.4	108.215
15.6	107.219
10.7	104.770
8.6	104.038
5.8	103.779
1.4	102.183
four lead wires, circuit rebuilt, r = 0.9999	
15.2	106.121
10.4	104.510
6.5	103.033
0.7	100.954
-2.7	99.624
-7.1	98.109
-12.4	96.174
-15.5	95.074

FIGURE [3-2]

Temperature dependence of Pt resistor

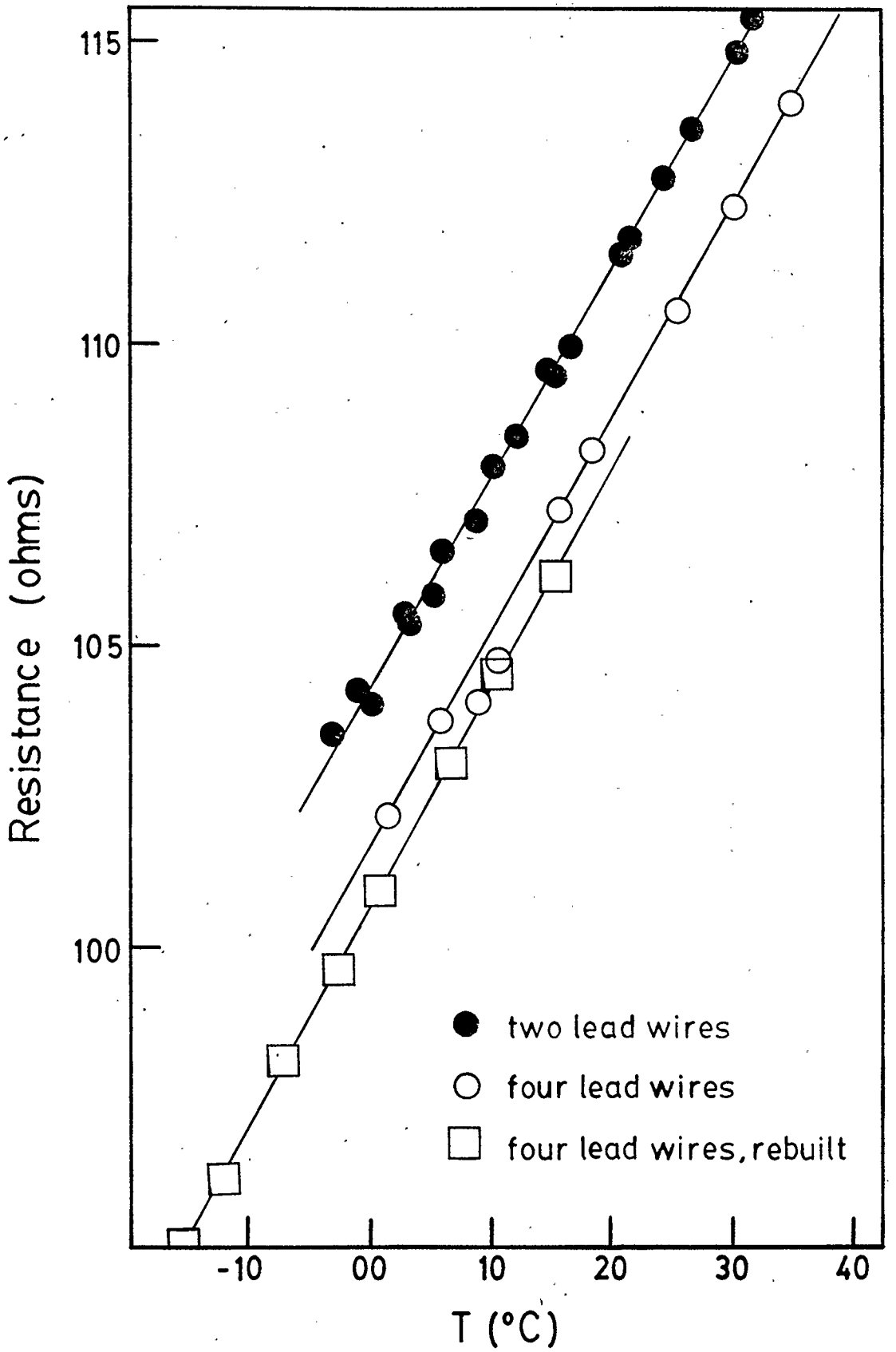
115
110
105
100
Resistance (ohms)
-10
00
10
20
30
40
T (°C)
two lead wires
four lead wires
four lead wires, rebuilt

$$T(°C) = (2.76 \pm 0.01)R(\Omega) - (278.00 \pm 1.30) \qquad [3\text{-}1c]$$

The metal pressure vessel decreases the homogeneity of the magnetic field, which gives rise to an increased broadening of the NMR linewidth that must be taken into account. This was done by determining the dependence of the pure acetonitrile linewidth on temperature in the high pressure vessel and comparing with the temperature dependence in the normal probehead.

3.2 Acetonitriletris(2-aminoethyl)aminecopper(II) Perchlorate and Acetonitriletris(N,N',N"-dimethyl-2-aminoethylaminecopper(II) Perchlorate

The hexakisacetonitrilecopper(II) perchlorate complex was prepared, using the procedure of van Leeuwen and Groenveld,[78] from hydrated copper perchlorate. To a warm acetonitrile solution of $Cu(CH_3CN)_6(ClO_4)_2$, the quadridentate ligand, tris(2-aminoethyl)amine ("tren"; Fluka A.G., > 97%, used as received) was added. The solution was heated to remove excess solvent and a light blue precipitate was filtered off. The precipitate was recrystallized from fresh acetonitrile and dried on a sintered glass funnel by allowing dry nitrogen to pass through it. Elemental analysis gave: C, 21.04%; H, 5.54%; N, 16.32% with expected values of C, 21.37%; H, 4.71%; N, 15.57%. The (acetonitrile)tris-(N,N',N"-dimethyl-2-aminoethyl)amine-copper(II) perchlorate, $[Cu(Me_6tren)CH_3CN](ClO_4)_2$, was obtained from Dr. S.F. Lincoln.

The UV-visible spectra for these complexes show an absorbance at 776 nm for the $[Cu(tren)CH_3CN](ClO_4)_2$ complex and at 848 nm for the $[Cu(Me_6tren)CH_3CN](ClO_4)_2$ complex. A Beer's law study of absorbance

versus concentration, for $[Cu(tren)CH_3CN](ClO_4)_2$ and $[Cu(Me_6tren)-CH_3CN](ClO_4)_2$, gave a straight line dependence [Figures [3-3] and [3-4]], r = 0.999, with molar absorbances of 146.8 ± 1.5 and 585.3 ± 2.9 $l\ mol^{-1}\ cm^{-1}$ respectively. These values are similar to those previously reported.[49]

For comparison purposes, the diamagnetic complex $[Zn(tren)CH_3CN]-(ClO_4)_2$ was prepared by the same procedure, giving a white crystalline solid. Elemental analysis: C, 21.01%; H, 5.25%; N, 15.70%; expected values are: C, 21.29%; H, 4.69%; N, 15.52%.

The temperature dependence of the acetonitrile linewidth was studied with a series of solutions, differing in concentration. The temperature dependence of the ^{14}N linewidth, in the presence of $[Cu(tren)CH_3CN]^{2+}$, was also studied with excess perchlorate ion, in the form of sodium perchlorate, added to the solutions. The variable pressure experiments were done either with the solutions from the variable temperature study or with freshly made solutions.

3.3 Bisacetonitrile(1,4,8,11-tetraazacyclotetradecane)nickel(III) Perchlorate and Trifluoromethanesulphonate

Hexaaquanickel(II) perchlorate was dissolved in ethanol (50 ml) and added to an ethanol solution of 1,4,8,11-tetraazacyclotetradecane (cyclam), forming a bright orange precipitate. This precipitate was recrystallized from water, with a small amount of perchloric acid added, to give orange crystals of $[Ni(cyclam)](ClO_4)_2$. Elemental analysis gave: C, 26.52%; H, 5.44%; N, 12.06% for calculated values of C, 26.63%; H, 5.28%; N, 12.73%.

FIGURE [3-3]

Beer's law plot of $[Cu(tren)CH_3CN]^{2+}$ in CH_3CN

at λ = 776 nm

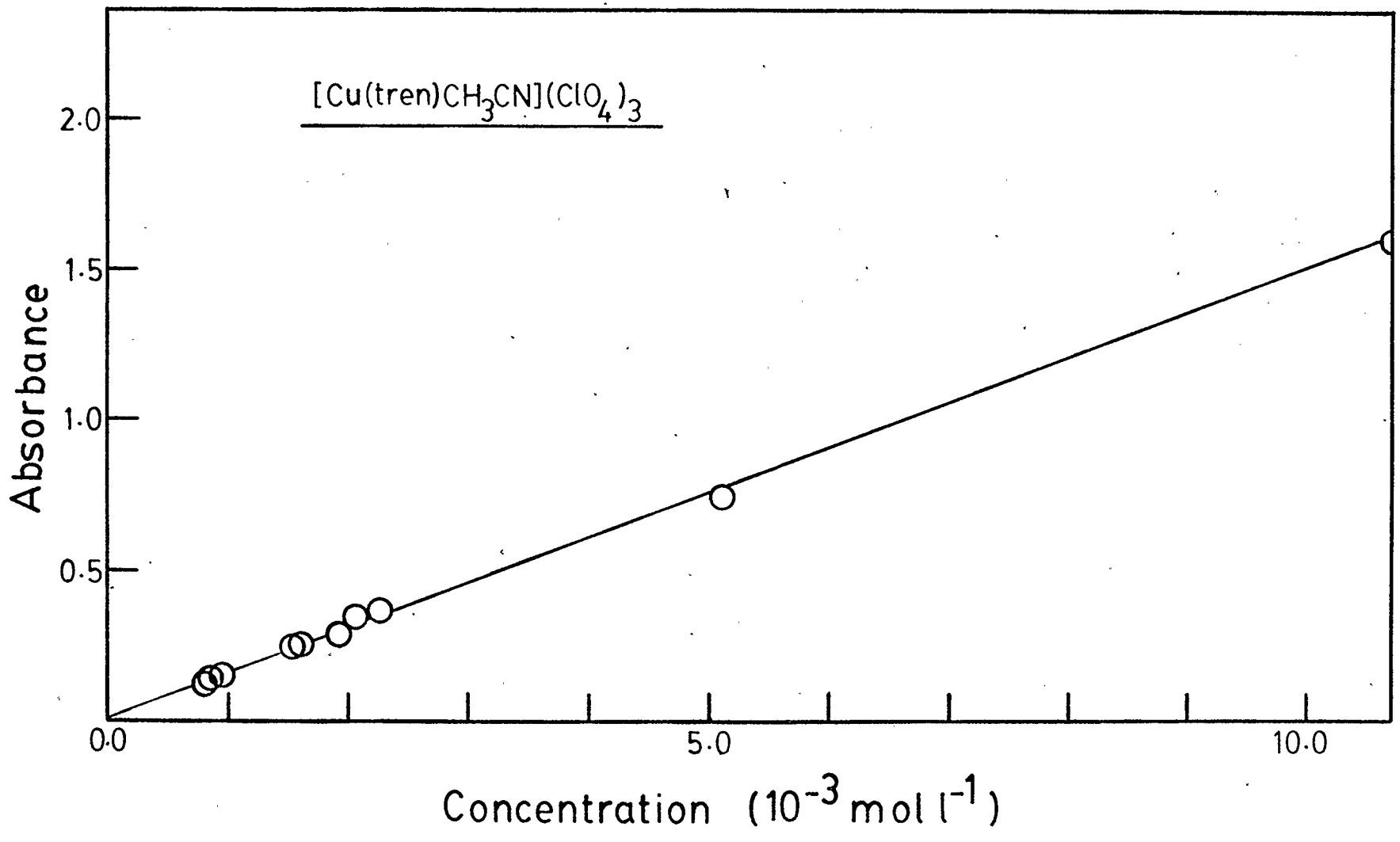
[Cu(tren)CH3CN](ClO4)3
Absorbance
2.0
1.5
1.0
0.5
0.0
5.0
10.0
Concentration (10-3 mol l-1)

FIGURE [3-4]

Beer's law plot of $[Cu(Me_6tren)CH_3CN]^{2+}$ in CH_3CN

at λ = 848 nm

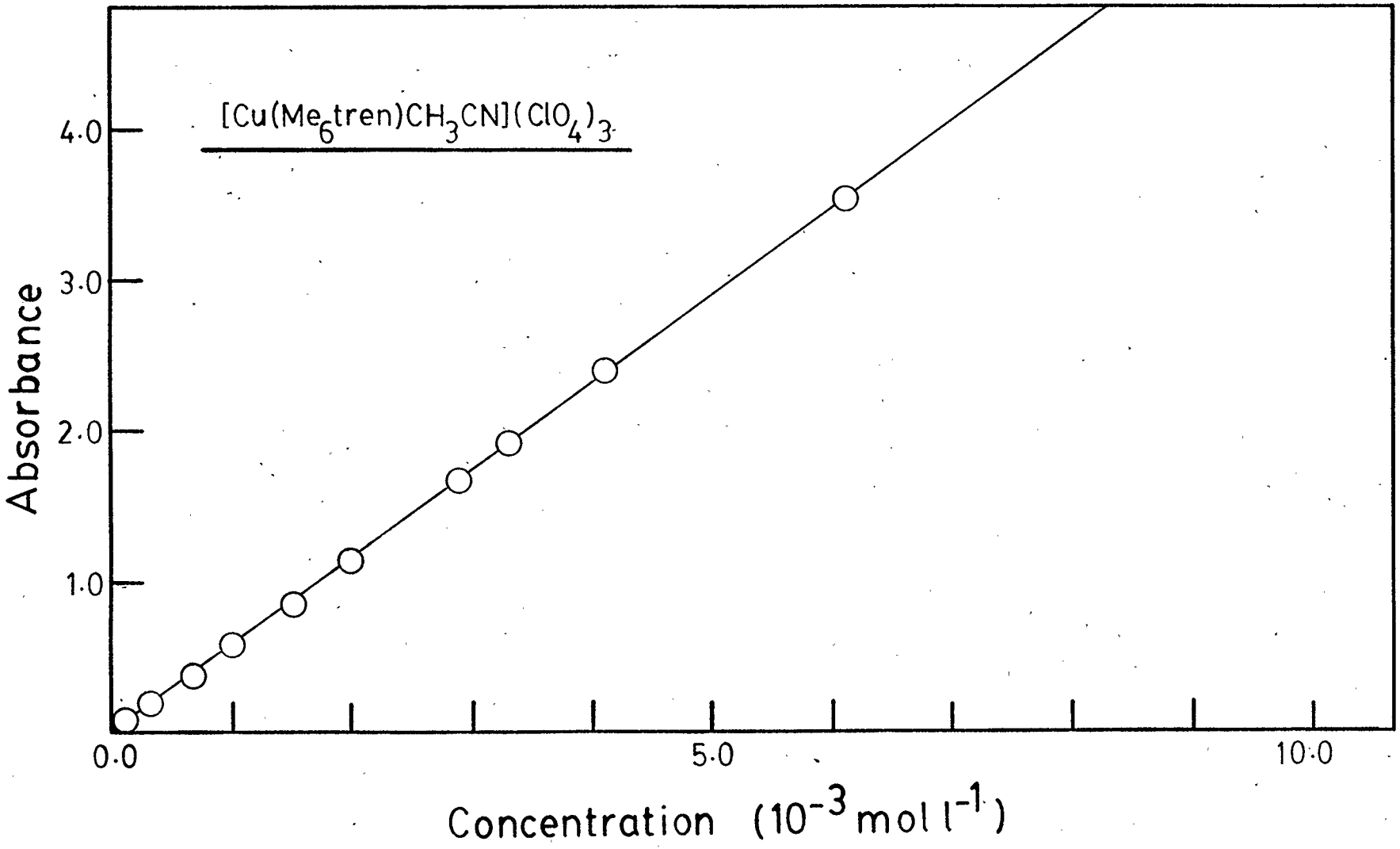
[Cu(Me6tren)CH3CN](ClO4)3
Absorbance
4·0
3·0
2·0
1·0
0·0
5·0
10·0
Concentration (10-3 mol l-1)

A solution of $[Ni(cyclam)](ClO_4)_2$ in dry acetonitrile was placed in both sides of a redox cell (Figure [3-5]) with anhydrous sodium perchlorate as a supporting electrolyte (0.1 mol l^{-1}). A low current (10 mA, 4 V) was applied using platinum wire electrodes, giving a dark olive-green solution in the oxidation side and a dark red solution in the reduction side. Evaporation of the solution from the oxidation side gave $[Ni(cyclam)(CH_3CN)_2](ClO_4)_3$ as a dark green powder. Elemental analysis gave: C, 26.68%; H, 5.24%; N, 12.83% for calculated values of C, 26.30%; H, 4.73%, N, 13.14%.

The complex $[Ni(cyclam)(CH_3CN)_2][CF_3SO_3]_3$ was prepared in the same manner from the $Ni(CF_3SO_3)_2$ salt, using $NaCF_3SO_3$ as a supporting electrolyte, producing dark green crystals. Elemental analysis gave: C, 26.34%; H, 4.36%; N, 11.02% for calculated values of C, 25.90%, H, 3.84%; N, 10.66%.

The $[Ni(cyclam)](ClO_4)_2$ complex absorbs light at 458 and 322 nm. The linear dependence of absorbance on the concentration (Figure [3-6]), $r = 0.9996$, gives the molar absorbance as 14.69 ± 0.18 and 14.06 ± 0.20 l mol^{-1} cm^{-1} respectively. Previous studies[70,80] show that the $[Ni(cyclam)]^{2+}$ complex in water absorbs light at 448 nm with a maximum value of 65 ± 1 l mol^{-1} cm^{-1} for the molar absorbance. This value is affected by the equilibrium between the high spin and low spin form of the complex, and is dependent on the amount of electrolyte and the temperature of the solution.[80] $[Ni(cyclam)(CH_3CN)_2](ClO_4)_3$ absorbs at 365 and 308 nm. Unfortunately the absorbance data are very scattered (Figure [3-7]) and the largest molar absorbance obtained is approximately 1100 l mol^{-1} cm^{-1} at 308 nm, which is 10% of the previously reported value.[65,69,81] This suggests that the major species

FIGURE [3-5]

Reduction-oxidation cell

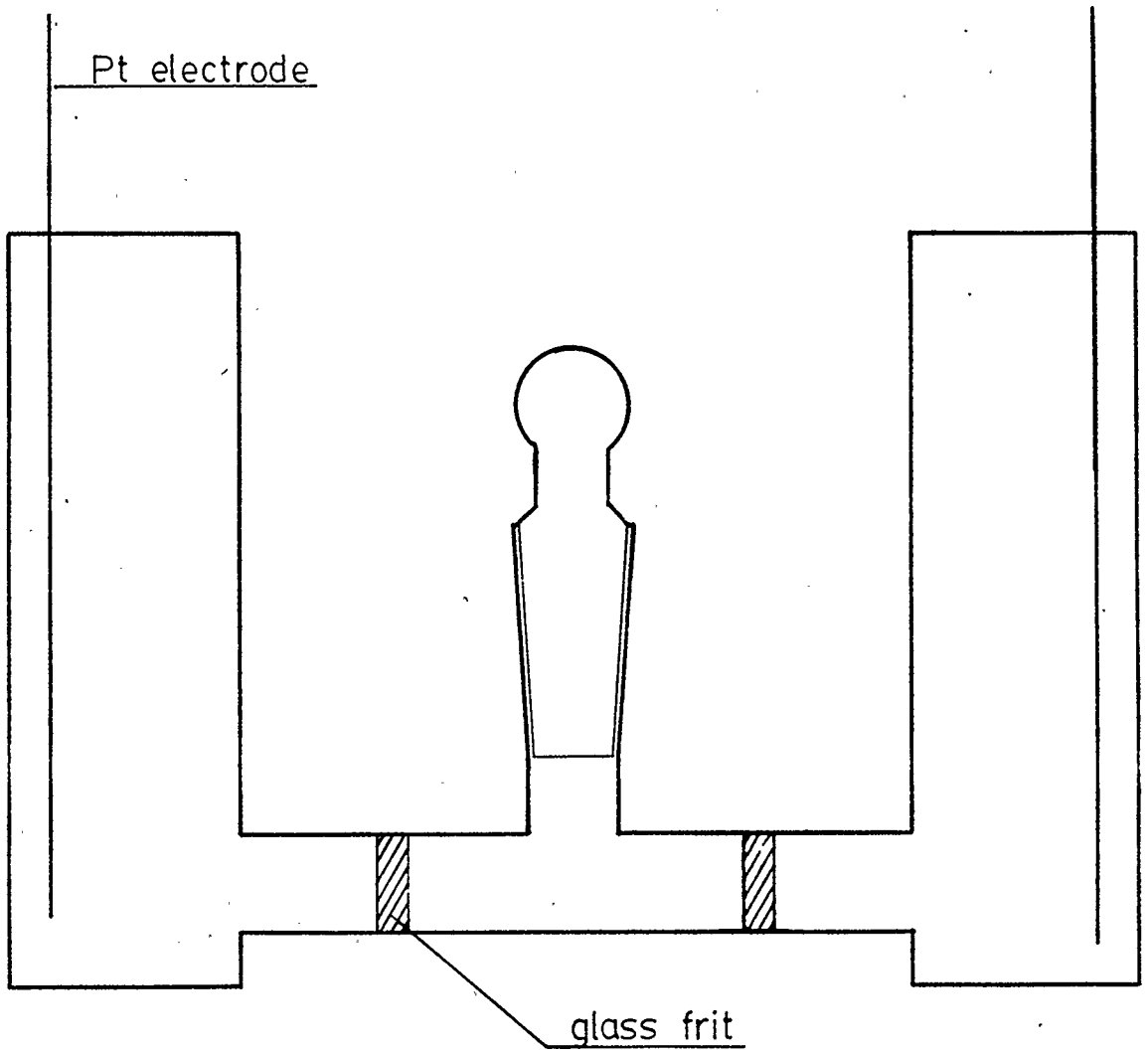
Pt electrode
glass frit

FIGURE [3-6]

Beer's law plot of $[Ni(cyclam)]^{2+}$ in CH_3CN

at λ = 458 and 322 nm

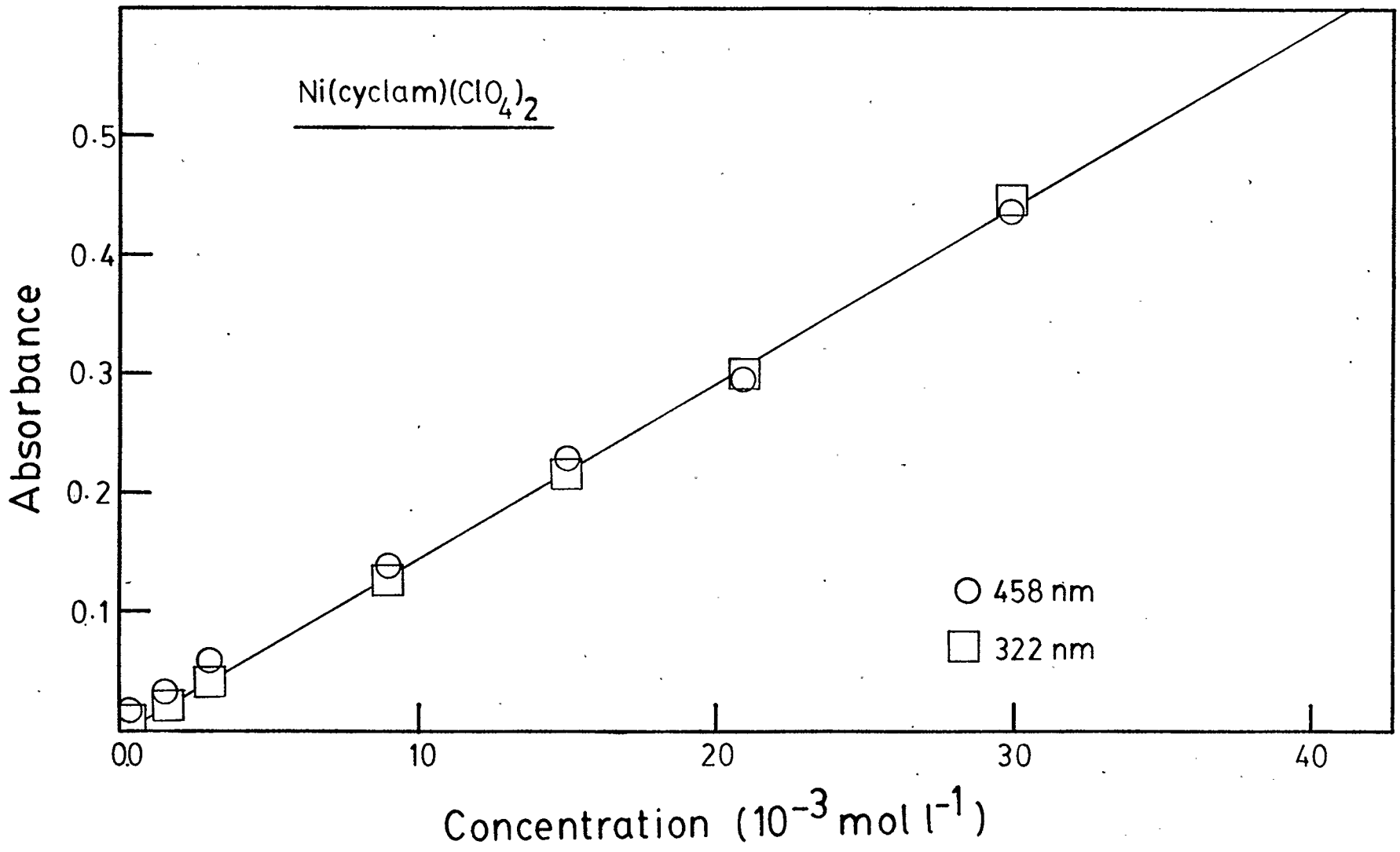
Ni(cyclam)(ClO4)2
Absorbance
0.5
0.4
0.3
0.2
0.1
0.0
10
20
30
40
Concentration (10-3 mol l-1)
458 nm
322 nm

FIGURE [3-7]

Beer's law plot of $[Ni(cyclam)(CH_3CN)_2]^{3+}$ in CH_3CN

at λ = 365 and 308 nm

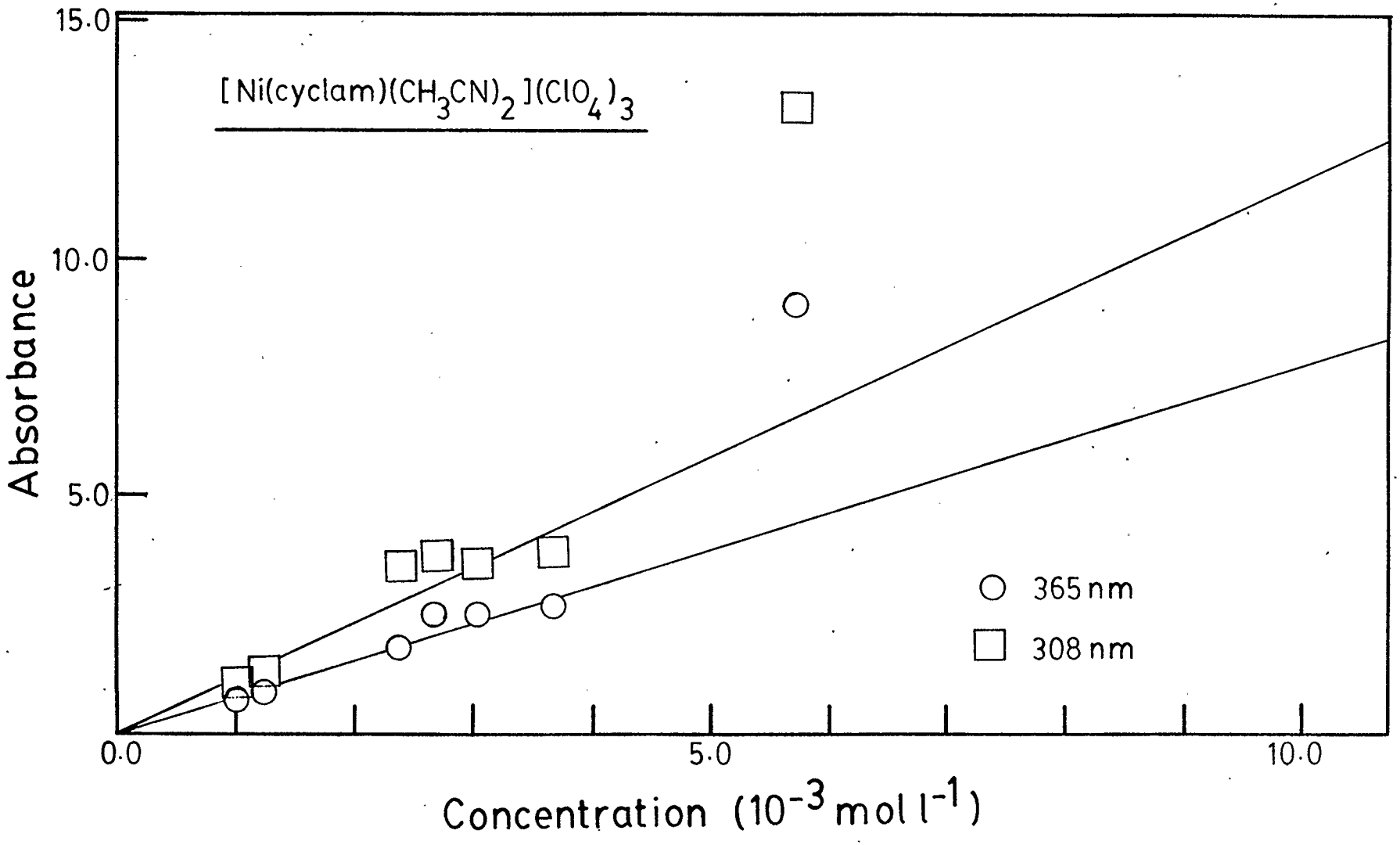
15·0
10·0
5·0
0·0
5·0
10·0
Absorbance
[Ni(cyclam)(CH3CN)2](ClO4)3
365 nm
308 nm
Concentration (10-3 mol l-1)

in solution is not $[Ni(cyclam)(CH_3CN)_2]^{3+}$ but $[Ni(cyclam)]^{2+}$ in equilibrium with the high spin form, $[Ni(cyclam)(CH_3CN)_2]^{2+}$, with only a maximum of 10% of the more highly oxidized complex present. The $[Ni(cyclam)(CH_3CN)_2](CF_3SO_3)_3$ solutions prepared had light absorption maxima at 468 and 321 nm, which suggests that all of the complex present had been reduced on dissolution and was actually present as $[Ni(cyclam)](CF_3SO_3)_2$.

It appears that the main species in the solutions was the less oxidized nickel(II) complex and therefore the increased ^{14}N relaxation of CH_3CN, described below, could be due to the chemical exchange of the solvent on the high spin form of the Ni(II) compound. The equilibrium between low spin and high spin $[Ni(cyclam)](ClO_4)_2$ was studied using the temperature dependence of the UV-visible spectra of the complex in CH_3CN.

The diamagnetic complex $[Co(cyclam)(CH_3CN)_2](ClO_4)_3$ was made for comparison purposes. The green complex $[Co(cyclam)Cl_2]Cl$ was made using the procedure of Bosnich et al.[79] An aqueous solution of this complex was passed through an anion exchange column (Dowex 1-X4, OH^- form) producing dark red $[Co(cyclam)(OH)_2]OH$. Perchloric acid (70%) was then added dropwise, until the solution was slightly acidic, producing dark green $[Co(cyclam)(H_2O)_2](ClO_4)_3$. The excess water was evaporated off and the dark green crystals were then dissolved in dry acetonitrile. The remaining water was removed by adding triethylorthoformate (a drying agent)[78] producing an orange solution that gave $[Co(cyclam)(CH_3CN)_2](ClO_4)_3$ as an orange powder when the solvent was evaporated. Elemental analysis gave: C, 26.22%; H, 4.90%; N, 14.30% for calculated values of C, 26.29%, H, 4.73%; N, 13.14%. An acetonitrile solution of

$[Co(cyclam)(CH_3CN)_2](ClO_4)_3$ absorbs light at 437 nm with a molar absorbance of 78.5 l mol^{-1} cm^{-1}.

Solutions of these nickel complexes, used for the variable temperature and pressure NMR experiments were made fresh and sealed in either a 5 mm NMR tube or the high pressure probe.

Chapter 4 Experimental Results

4.1 Acetonitrile Alone

The variable temperature studies of pure CH_3CN (Table [4-1]) give the temperature dependence of the ^{14}N transverse relaxation time, T_2 (= $T_1 = 1/\pi\ \nu_{1/2}$). This dependence is shown in Figure [4-1] as a straight line (correlation coefficient r = 0.9993) which can be described by equation [4-1]. From this can be calculated an activation energy, $E_\perp$ = 7.40 ± 0.06 kJ mol^{-1}, for diffusion by rotation perpendicular to the C_{3v} axis of the molecule.

$$\ln T_1 = -(2.548 \pm 0.026) - (890 \pm 8)/T \qquad [4\text{-}1]$$

This is in good agreement with previous reports.[73-75] A similar variable temperature study in the high pressure probehead indicated that the presence of the pressure vessel increases the ^{14}N NMR linewidth by 12 Hz by decreasing the homogeneity of the magnetic field.

The pressure dependence of T_1 is described by equation [4-2], where $\Delta V_\perp^*$ is the volume of activation for diffusion by rotation perpendicular to the C_{3v} axis of the solvent molecule.

$$(\partial \ln T_1/\partial P)_T = (\partial \ln D_1/\partial P)_T \simeq \ln(D_\perp/D_\perp{}^0)/P = \Delta V_\perp^*/RT \qquad [4\text{-}2]$$

The variable pressure results (Table [4-2]) as shown in Figure [4-2] indicate that, within experimental error, ΔV^* is independent of pressure and temperature. The linear relationship between $T\ln(D_\perp/D_\perp{}^0)$ and P, (r = 0.9904), gives ΔV^* = 6.2 ± 0.12 $cm^3\ mol^{-1}$. This value is in excellent agreement with previously obtained results.[36,73]

TABLE [4-1]

Temperature dependence of the ^{14}N relaxation time T_1 (= T_2) of pure acetonitrile

$10^3/T$ (K^{-1})	ln T_1
3.526	-5.676
3.800	-5.934
4.125	-6.227
4.295	-6.372
3.963	-6.078
3.675	-5.802
3.302	-5.475
3.074	-5.280
3.194	-5.427
3.251	-5.448
3.039	-5.255
3.145	-5.351
3.101	-5.310
2.902	-5.150
2.825	-5.076
3.294	-5.470
3.059	-5.266
2.898	-5.115
2.996	-5.197
3.181	-5.367
3.524	-5.710

FIGURE [4-1]

Temperature dependence of the ^{14}N longitudinal relaxation time T_1 (= T_2) of pure acetonitrile

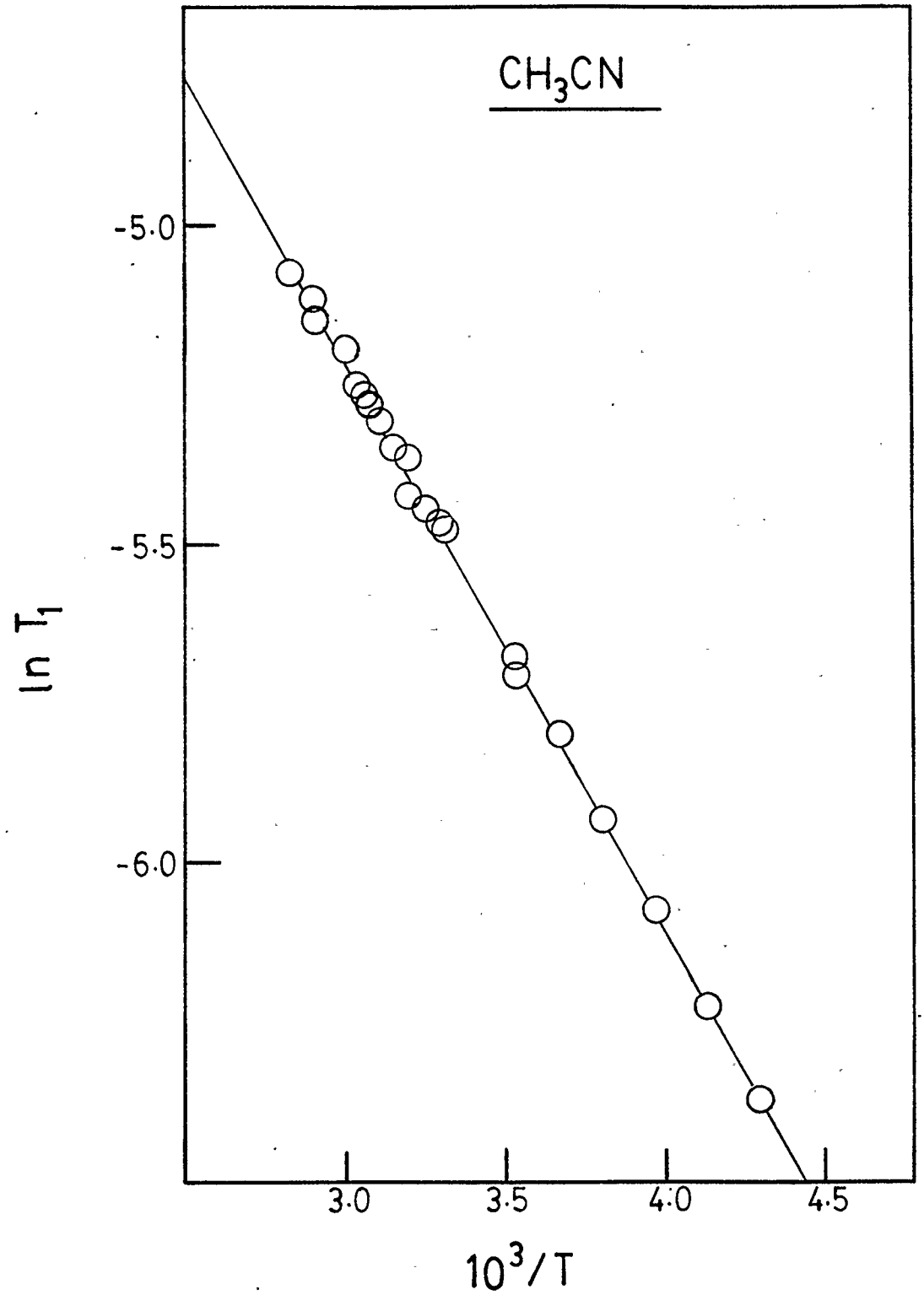
CH3CN
-5.0
-5.5
-6.0
ln T1
3.0
3.5
4.0
4.5
10^3/T

TABLE [4-2]

Pressure dependence of the diffusion coefficient

$D_\perp$ of pure acetonitrile, 18.0 > T > -15.0°C

P(Mpa)	T $\ln(D_\perp/D_\perp^0)$	P(MPa)	T $\ln(D_\perp/D_\perp^0)$
T = 17.5°C		T = -5.6°C	
0.1	2.073	0.1	3.48
82.2	-55.487	82.2	-62.60
164.1	-199.151	161.6	-119.57
200.0	-119.442	202.4	-156.76
121.5	-87.473	119.2	-85.87
40.7	-36.309	39.4	-38.79
0.2	-9.631	2.6	5.36
T = -14.0°C		60.2	-60.19
0.1	0.774	191.8	-147.85
82.6	-70.222	148.8	-108.87
160.8	-130.856	52.1	-40.39
202.6	-155.731	1.8	2.14
118.0	-90.174		
40.0	-27.467		
1.2	-3.887		
203.3	-156.249		
177.0	-135.520		
22.4	-21.248		
0.1	-6.219		

FIGURE [4-2]

Pressure dependence of the diffusion coefficient $D_{\perp}$ of pure acetonitrile, $18.0 > T > -15.0°C$

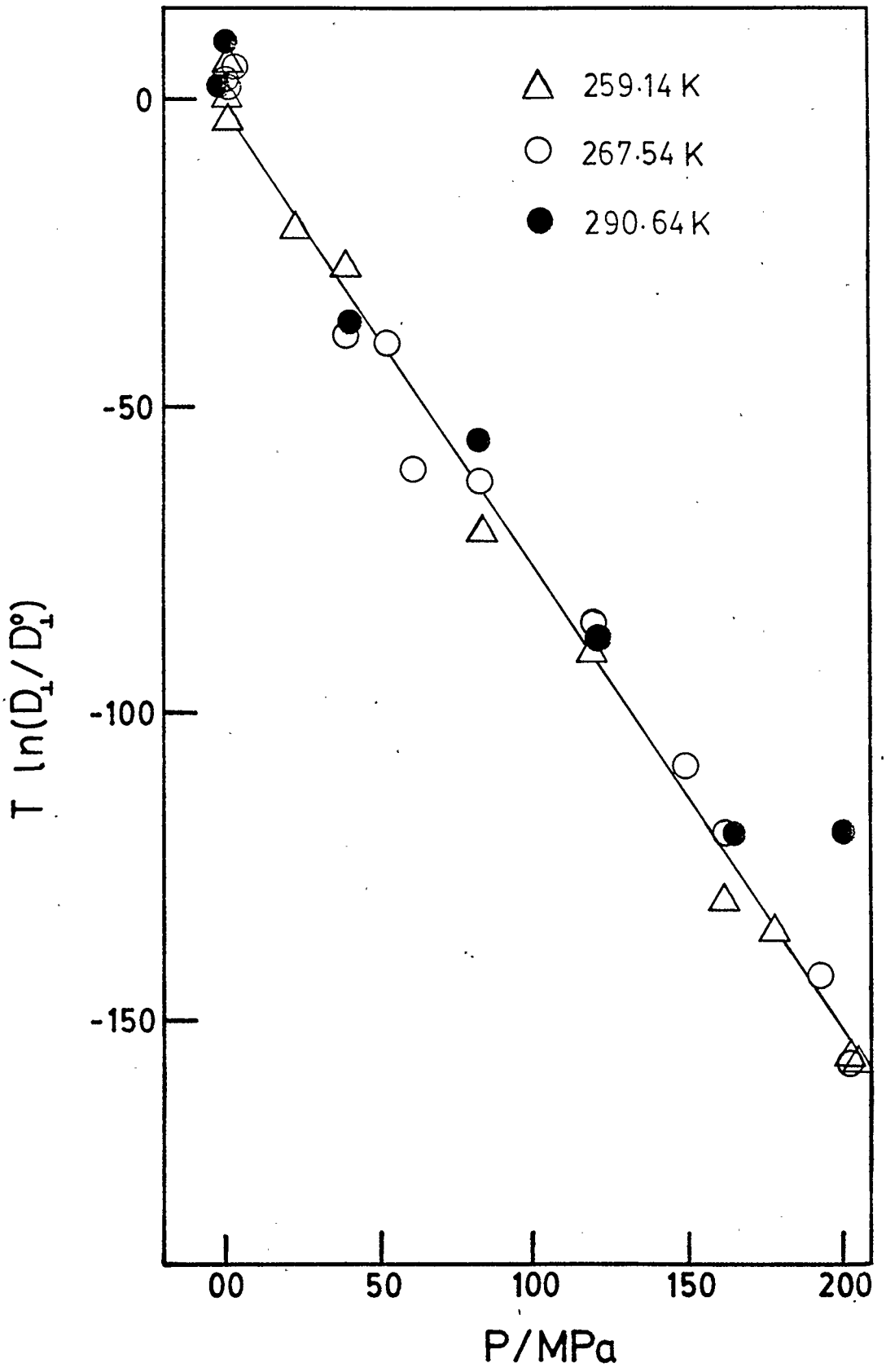
259.14 K
267.54 K
290.64 K
0
-50
-100
-150
T ln(D_t/D_t°)
00
50
100
150
200
P/MPa

4.2 Acetonitriletris(2-aminoethyl)aminecopper(II) Perchlorate in Acetonitrile

The $[Cu(tren)(CH_3CN)]^{2+}$ complex contributes to the ^{14}N relaxation of CH_3CN primarily through the slow exchange process, with some minor contributions from the fast exchange and the outer sphere relaxation processes. The temperature dependence of the ^{14}N relaxation was studied for three concentrations (Table [4-3]) as shown in Figure [4-3]. The data indicate that $(P_mT_{2p})^{-1}$ is essentially equal to the solvent exchange rate constant, k_{ex}, over the temperature range 4.6 to 39.4°C, but that k_{ex} is dependent on the solute concentration varying from 1.02×10^6 to 0.181×10^6 s^{-1}, at 25°C, for 2.023×10^{-3} and 13.78×10^{-3} mol kg^{-1} $[Cu(tren)CH_3CN](ClO_4)_2$ respectively. The term, P_mT_{2p}, is dependent on the ClO_4^- ion concentration as shown by the addition of $NaClO_4$ to a solution containing the $[Cu(tren)CH_3CN]^{2+}$ ion (Table [4-4], Figure [4-4]). For a 1.18×10^{-3} mol kg^{-1} solution of $[Cu(tren)(CH_3CN)](ClO_4)_2$, the rate constant at 25°C varies from 0.684×10^6 to 0.36×10^6 s^{-1} upon the addition of 0.00 and 9.46×10^{-3} mol kg^{-1} $NaClO_4$ to the solution. The addition of $NaClO_4$ to pure CH_3CN (Table [4-5]) has no effect on the ^{14}N linewidth. The temperature dependence of the ^{14}N longitudinal relaxation, T_1 (= T_2), (Figure [4-5]) is given by the linear expression [4-3], r = 0.9983, in good agreement with the expression obtained for pure acetonitrile.

$$\ln T_1 = -(2.538 \pm 0.0363) - (897.16 \pm 10.75)/T \qquad [4\text{-}3]$$

The $[Zn(tren)(CH_3CN)](ClO_4)_2$ complex, a diamagnetic analogue of the copper complex, had no effect on the ^{14}N linewidth over the temperature

TABLE [4-3]

Temperature dependence of $(P_m T_{2p})^{-1}$ for

$[Cu(tren)CH_3CN](ClO_4)_2$ in CH_3CN

$10^3/T$ (K^{-1})	$-\ln(P_m T_{2p})$
2.023×10^{-3} mol kg^{-1}	
3.725	12.607
3.890	12.215
3.950	12.338
3.292	14.175
3.245	14.234
3.187	14.234
3.231	14.292
3.266	14.040
3.513	13.200
3.614	12.830
3.597	12.939
3.479	13.577
3.091	14.578
2.902	14.983
2.742	15.063
2.835	15.038
3.661	13.121
3.958	12.580
3.746	12.636
3.518	13.380
6.553×10^{-3} mol kg^{-1}	
4.208	11.271
3.300	13.146
3.089	13.622
2.911	14.020
2.761	14.175
2.832	14.144
2.986	13.890
3.298	13.131
3.081	13.668
2.903	13.963
2.744	14.174

$10^3/T$ (K^{-1})	$-\ln(P_m T_{2p})$
1.378×10^{-2} mol kg^{-1}	
4.023	11.022
4.206	10.975
3.095	12.774
3.004	12.881
2.919	13.331
3.300	12.092
3.089	12.914
2.911	13.532
2.761	13.733
2.832	13.580
2.986	13.199
3.298	12.298
3.081	12.964
2.903	13.338
2.744	13.672

FIGURE [4-3]

Temperature dependence of $(P_m T_{2p})^{-1}$ for

$[Cu(tren)CH_3CN]^{2+}$ in CH_3CN

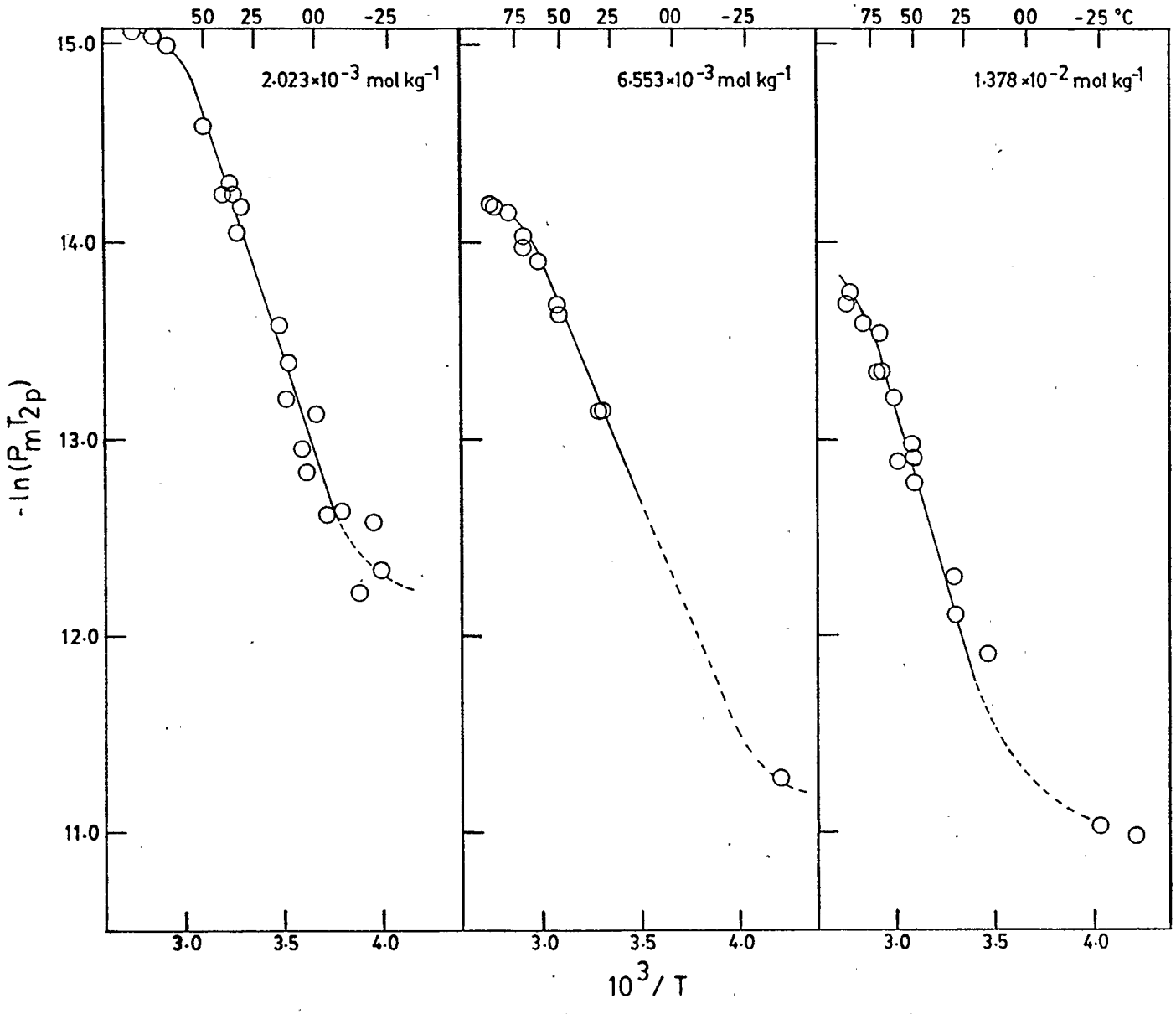
50 25 00 -25
75 50 25 00 -25
75 50 25 00 -25 °C
2·023×10⁻³ mol kg⁻¹
6·553×10⁻³ mol kg⁻¹
1·378×10⁻² mol kg⁻¹
15·0
14·0
13·0
12·0
11·0
-ln(P_m T_2p)
3·0
3·5
4·0
10³ / T

TABLE [4-4]

Temperature dependence of $(P_m T_{2p})^{-1}$ for

1.18×10^{-3} mol kg^{-1} $[Cu(tren)CH_3CN](ClO_4)_2$

in CH_3CN with $NaClO_4$ added

$10^3/T$ (K^{-1})	$-\ln(P_m T_{2p})$
0.00 mol kg^{-1} $NaClO_4$	
3.291	13.595
3.088	14.431
2.836	14.855
3.004	14.565
3.181	14.081
3.408	13.239
3.634	11.953
3.512	12.483
3.641	12.207
3.243	13.846
3.149	14.231
3.395	13.323
3.581	12.390
3.050	14.472
2.868	14.936
2.795	14.992
2.976	14.681
4.732×10^{-3} mol kg^{-1} $NaClO_4$	
3.243	13.617
3.153	13.935
3.395	12.702
3.452	12.766
3.581	11.679
3.881	11.788
3.846	12.065
3.051	14.221
2.868	14.685
2.797	14.900
2.976	14.435
9.463×10^{-3} mol kg^{-1} $NaClO_4$	
3.291	12.919
3.088	13.860
2.915	14.321
2.840	14.538
3.004	14.066
3.181	13.517
3.406	12.356
3.512	11.490
3.642	11.626
4.287	13.037
4.109	12.342

FIGURE [4-4]

Temperature dependence of $(P_m T_{2p})^{-1}$ for 1.18×10^{-3} mol kg^{-1} $[Cu(tren)CH_3CN]^{2+}$ in CH_3CN with $NaClO_4$ added

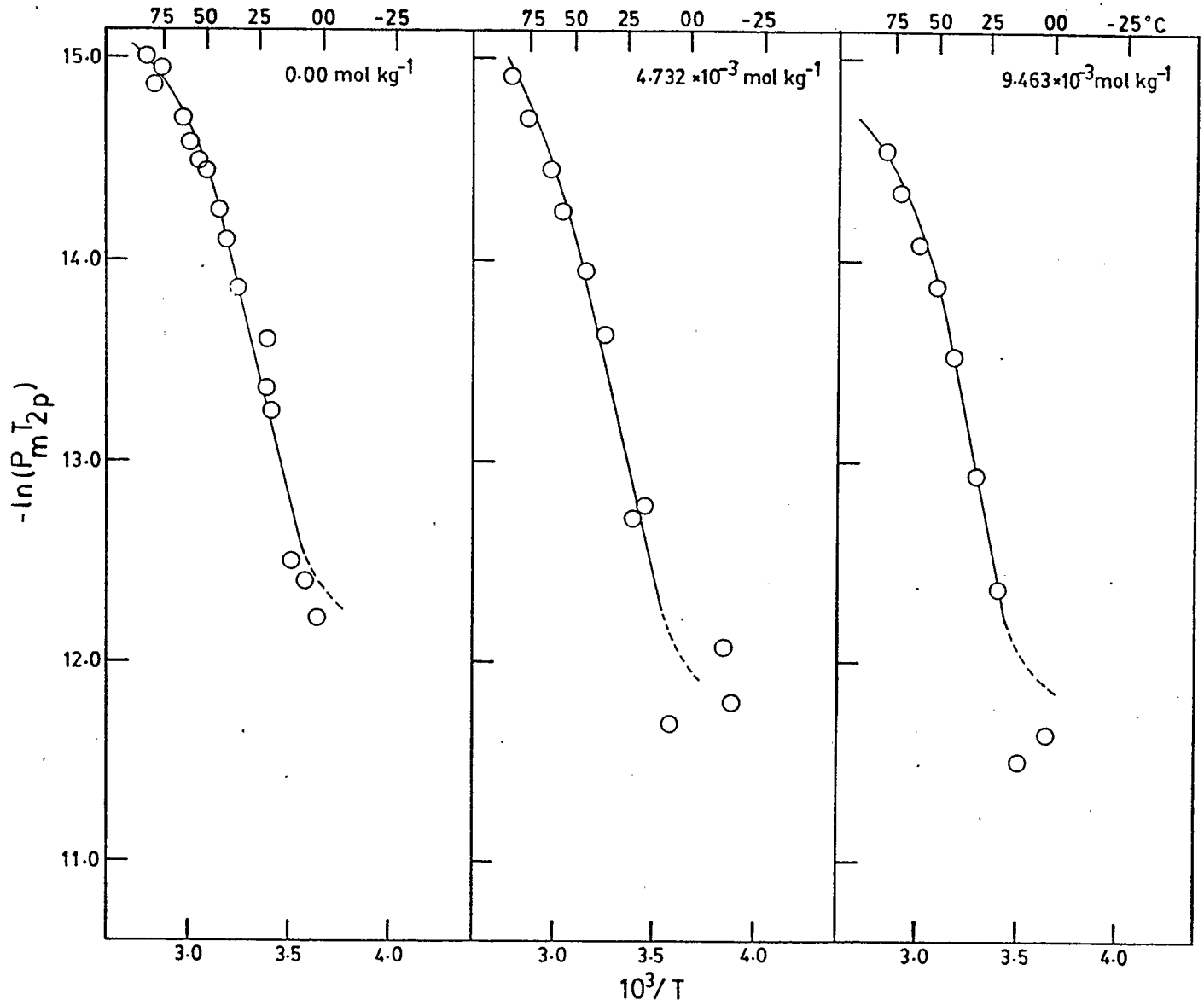
75 50 25 00 -25
75 50 25 00 -25
75 50 25 00 -25 °C
0·00 mol kg⁻¹
4·732 ×10⁻³ mol kg⁻¹
9·463×10⁻³mol kg⁻¹
15·0
14·0
13·0
12·0
11·0
-ln(P_m T_2p)
3·0
3·5
4·0
10³/ T

TABLE [4-5]

Temperature dependence of the ^{14}N longitudinal relaxation time T_1 (= T_2) for 1.157×10^{-2} mol kg^{-1} $NaClO_4$ in CH_3CN

$10^3/T$ (K^{-1})	ln T_1
3.526	-5.698
3.800	-5.953
4.125	-6.227
3.963	-6.120
3.675	-5.806
3.302	-5.528
3.074	-5.298
3.194	-5.407
3.251	-5.441
3.039	-5.269
3.145	-5.353
3.101	-5.328
2.902	-5.145
2.825	-5.063

FIGURE [4-5]

Temperature dependence of the ^{14}N longitudinal relaxation time T_1 (= T_2) for 1.157×10^{-2} mol kg^{-1} $NaClO_4$ in CH_3CN

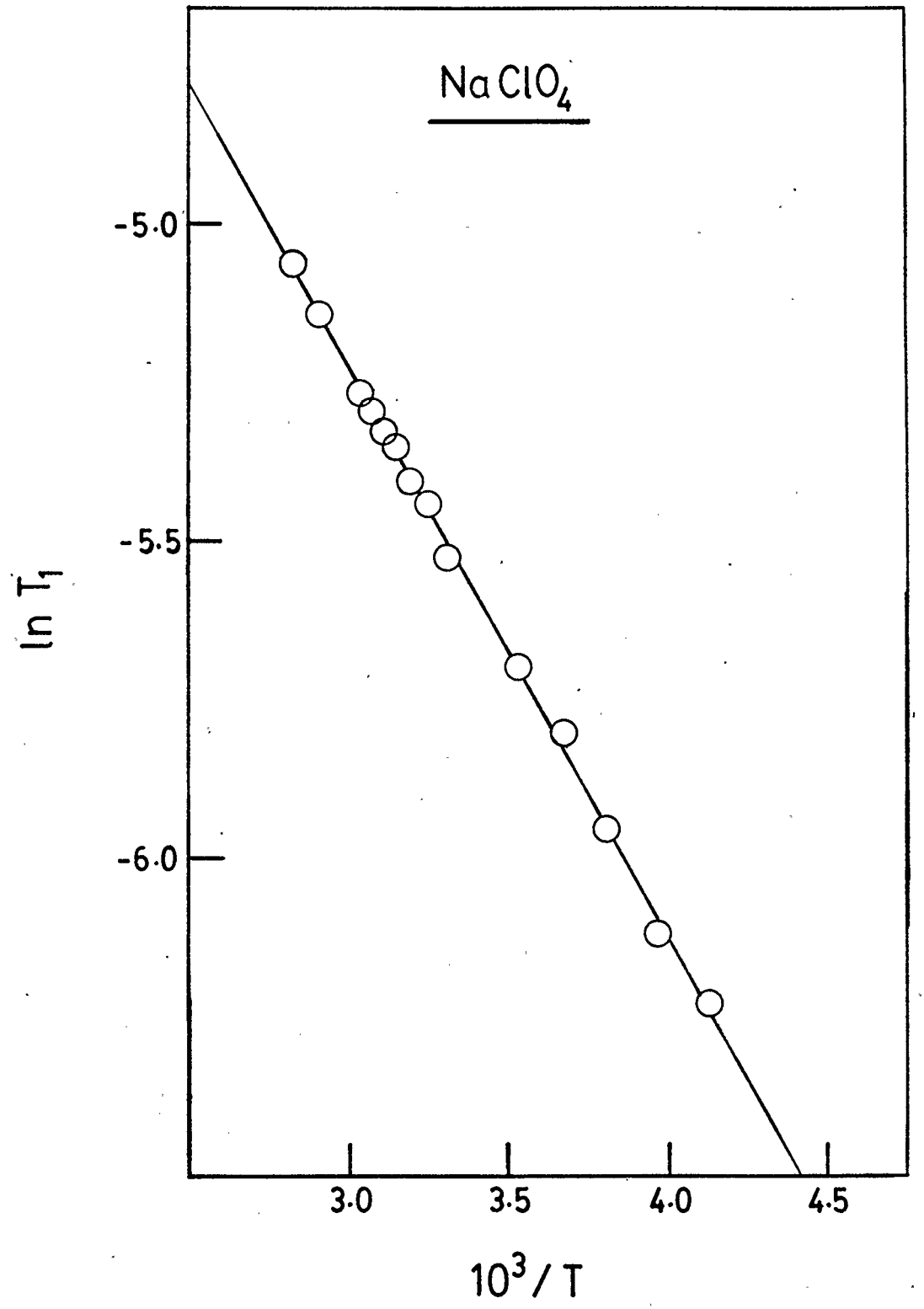
NaClO4
-5.0
-5.5
-6.0
ln T1
3.0
3.5
4.0
4.5
10^3 / T

range 90° > T > -30°C (Table [4-6]). The temperature dependence of T_2 (= T_1) for a 3.091 x 10^{-3} mol kg^{-1} solution of $[Zn(tren)(CH_3CN)]^{2+}$, is shown in Figure [4-6] and is described by the straight line, r = 0.9986, equation [4-4].

$$\ln T_1 = -(2.538 \pm 0.0434) - (895.70 \pm 12)/T \qquad [4\text{-}4]$$

This result is identical with equation [4-1] within experimental uncertainty.

High pressure studies of the CH_3CN exchange on $[Cu(tren)CH_3CN]^{2+}$, at 15 and 30°C (Table [4-7]), show that the pressure dependence of the rate constant, k, (Figure [4-7]) cannot be written as the linear expression [4-5].

$$\ln k = -\ln(Pm\ T_{2p}) = -P\Delta V^*/RT \qquad [4\text{-}5]$$

At low pressures there is a large dependence of ln k on P with $\Delta V^* \simeq -30$ cm^3 mol^{-1}. As the pressure increases the slope decreases giving a limiting ΔV^* value of $\simeq -2$ cm^3 mol^{-1}.

4.3 Acetonitriletris(N,N',N"-dimethyl-2-aminoethyl)aminecopper(II) Perchlorate in Acetonitrile

The $[Cu(Me_6tren)CH_3CN]^{2+}$ complex contributes to the ^{14}N relaxation of CH_3CN solvent through the slow exchange and the outer sphere process. Variable temperature results (Table [4-8]) show a dependence on concentration similar to that noted for the $[Cu(tren)CH_3CN]^{2+}$ ion in solution (Figure [4-8]). Unfortunately the increase in the ^{14}N

TABLE [4-6]

Temperature dependence of the ^{14}N longitudinal relaxation time T_1 (= T_2) for 3.091×10^{-3} mol kg^{-1} $[Zn(tren)CH_3CN](ClO_4)_2$ in CH_3CN

$10^3/T$ (K^{-1})	ln T_1
3.294	-5.486
3.059	-5.252
2.898	-5.130
2.744	-5.023
3.177	-5.377
3.524	-5.702
3.812	-5.952
4.135	-6.285
4.276	-6.478
3.944	-6.079
3.653	-5.811

FIGURE [4-6]

Temperature dependence of the ^{14}N longitudinal relaxation time T_1 ($=T_2$) for 3.091×10^{-3} mol kg^{-1} $[Zn(tren)CH_3CN]^{2+}$ in CH_3CN

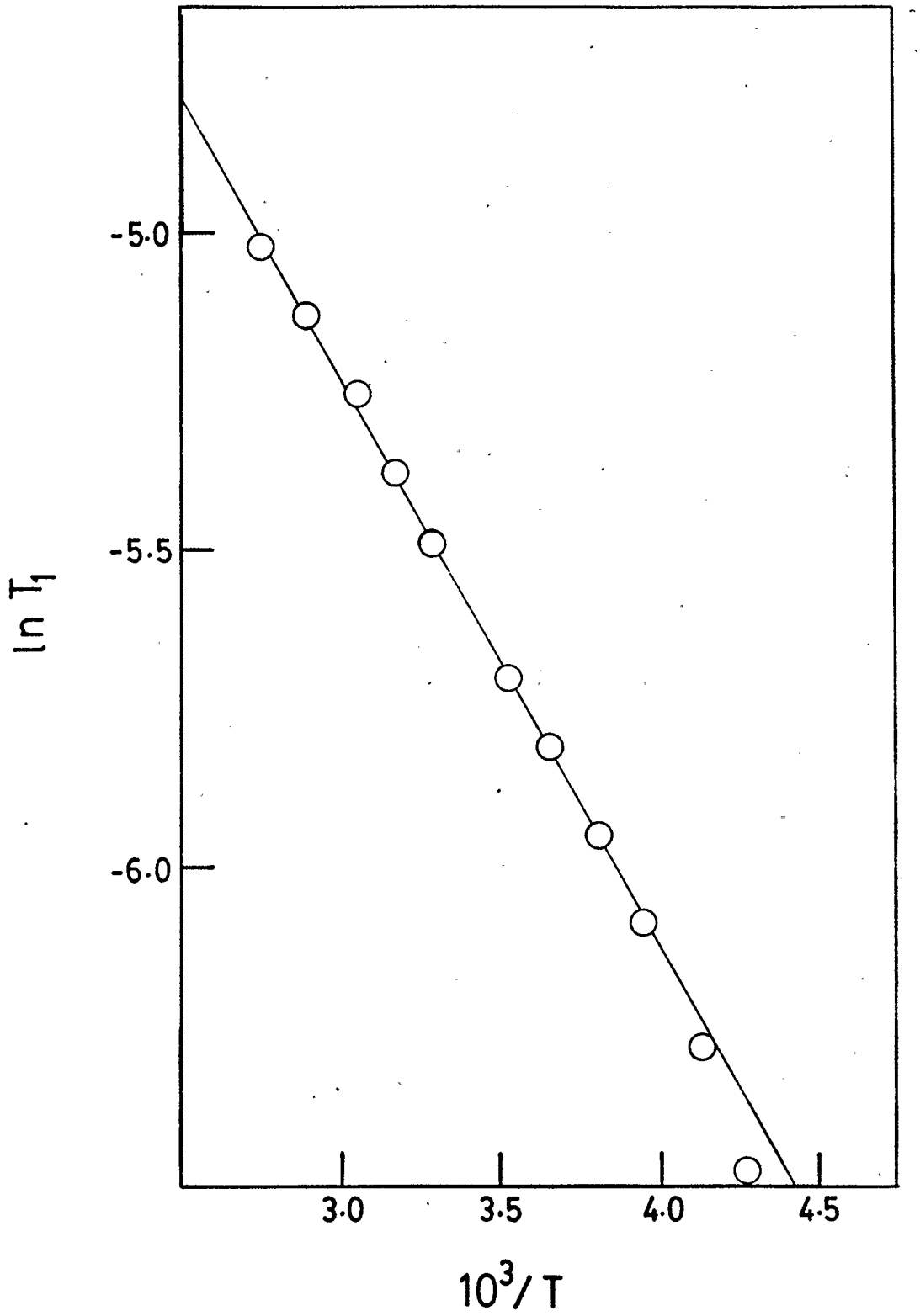
-5.0
-5.5
-6.0
ln T1
3.0
3.5
4.0
4.5
10³/ T

TABLE [4-7]

Pressure dependence of $(P_m T_{2p})^{-1}$ for

$[Cu(tren)CH_3CN](ClO_4)_2$ in CH_3CN

P(MPa)	$-\ln(P_m T_{2p})$
288.75 K, 2.067×10^{-3} mol kg^{-1}	
0.1	13.500
82.2	13.758
160.7	13.811
199.4	13.853
120.2	13.721
39.8	13.697
0.1	13.262
0.1	13.409
103.2	13.834
182.0	13.906
59.3	13.782
0.1	13.468
293.96 K, 2.067×10^{-3} mol kg^{-1}	
0.1	13.354
82.1	14.051
162.0	14.083
202.4	14.094
120.6	14.037
40.4	13.970
1.0	13.629
0.8	13.653
23.0	13.821
101.6	13.948
181.4	14.277
138.8	14.235
61.0	14.168
9.8	13.779
0.9	13.857

P(MPa)	$-\ln(P_m T_{2p})$
292.84 K, 2.493×10^{-3} mol kg^{-1}	
1.2	12.728
82.0	13.336
181.6	13.548
201.1	13.697
39.8	13.129
1.2	12.750
2.4	12.758
60.5	13.226
141.8	13.537
179.8	13.380
100.8	13.378
20.5	13.015
1.2	12.752

FIGURE [4-7]

Pressure dependence of $(P_m T_{2p})^{-1}$ for

$[Cu(tren)CH_3CN]^{2+}$ in CH_3CN

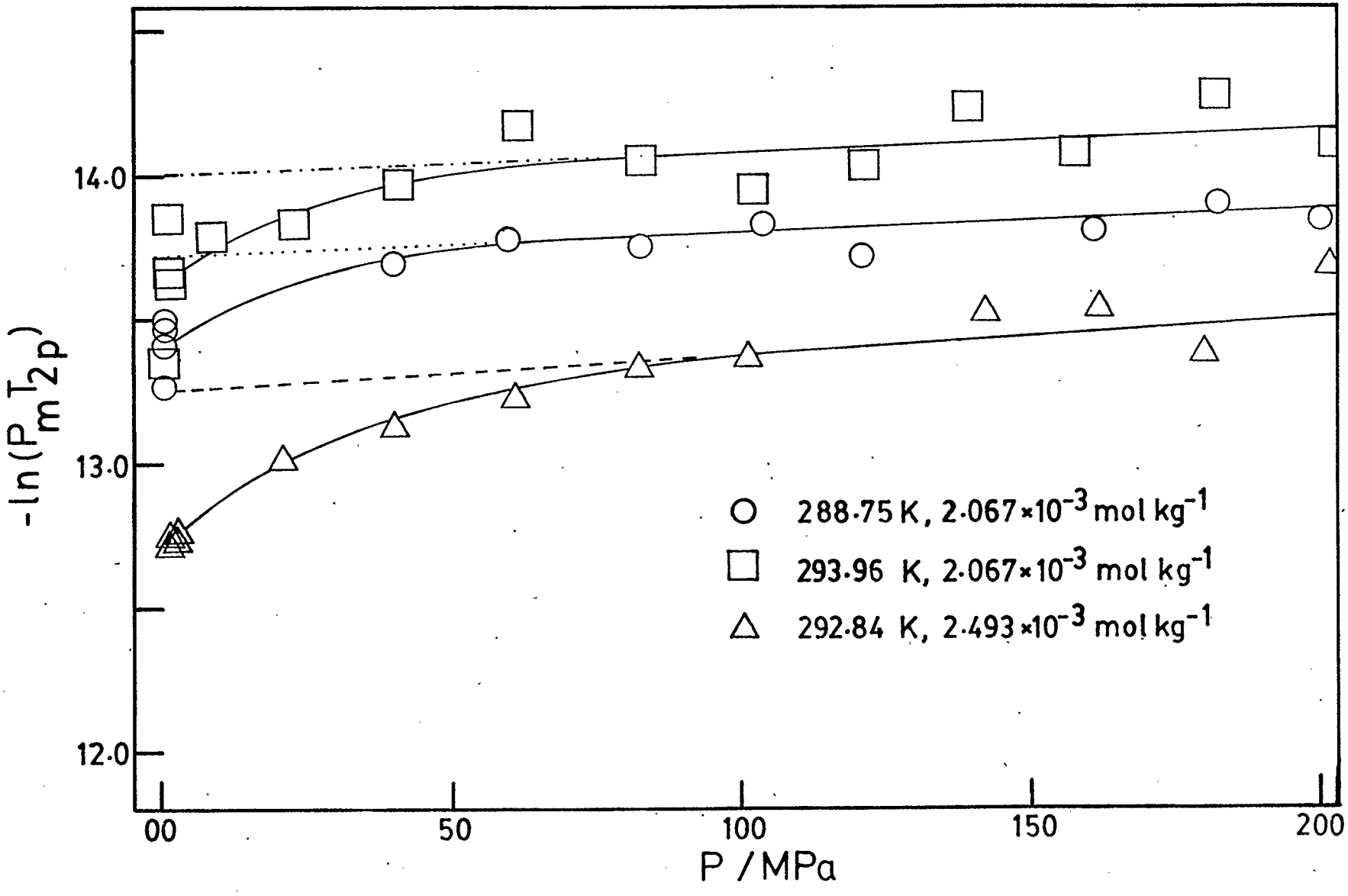
14·0
13·0
12·0
-ln(P_m T_2p)
00
50
100
150
200
P / MPa
288·75 K, 2·067×10⁻³ mol kg⁻¹
293·96 K, 2·067×10⁻³ mol kg⁻¹
292·84 K, 2·493×10⁻³ mol kg⁻¹

TABLE [4-8]

Temperature dependence of $(P_m T_{2p})^{-1}$ for

$[Cu(Me_6tren)CH_3CN](ClO_4)_2$ in CH_3CN

$10^3/T$	$-\ln(P_m T_{2p})$
3.732×10^{-3} mol kg^{-1}	
3.636	10.910
3.969	11.504
4.300	11.441
4.120	11.696
3.794	11.215
3.300	11.445
3.076	11.813
2.908	11.845
2.744	11.913
2.834	11.797
3.014	11.597
3.200	11.141
3.657	10.464
3.527	11.349
3.298	11.234
3.091	11.614
3.293	11.188
3.062	11.275
3.079	11.406
2.751	11.263
2.845	11.724
3.040	11.260
3.420	10.823
3.669	11.066
3.944	11.399
4.282	11.824
4.213	12.508
3.800	11.057

$10^3/T$	$-\ln(P_m T_{2p})$
5.277×10^{-3} mol kg^{-1}	
3.595	10.448
3.901	11.364
4.224	11.927
4.379	12.432
3.296	10.502
3.080	10.966
2.897	11.247
2.739	11.471
2.836	10.712
3.029	10.362
3.184	10.102
3.729	10.762
3.883	10.959
7.884×10^{-3} mol kg^{-1}	
3.595	10.830
3.901	10.970
4.224	11.133
4.379	11.316
3.296	10.565
3.080	10.895
2.897	11.027
2.739	11.261
2.836	11.102
3.029	10.904
3.184	10.451
3.729	10.452
3.883	10.654

FIGURE [4-8]

Temperature dependence of $(P_m T_{2p})^{-1}$ for

$[Cu(Me_6tren)CH_3CN]^{2+}$ in CH_3CN

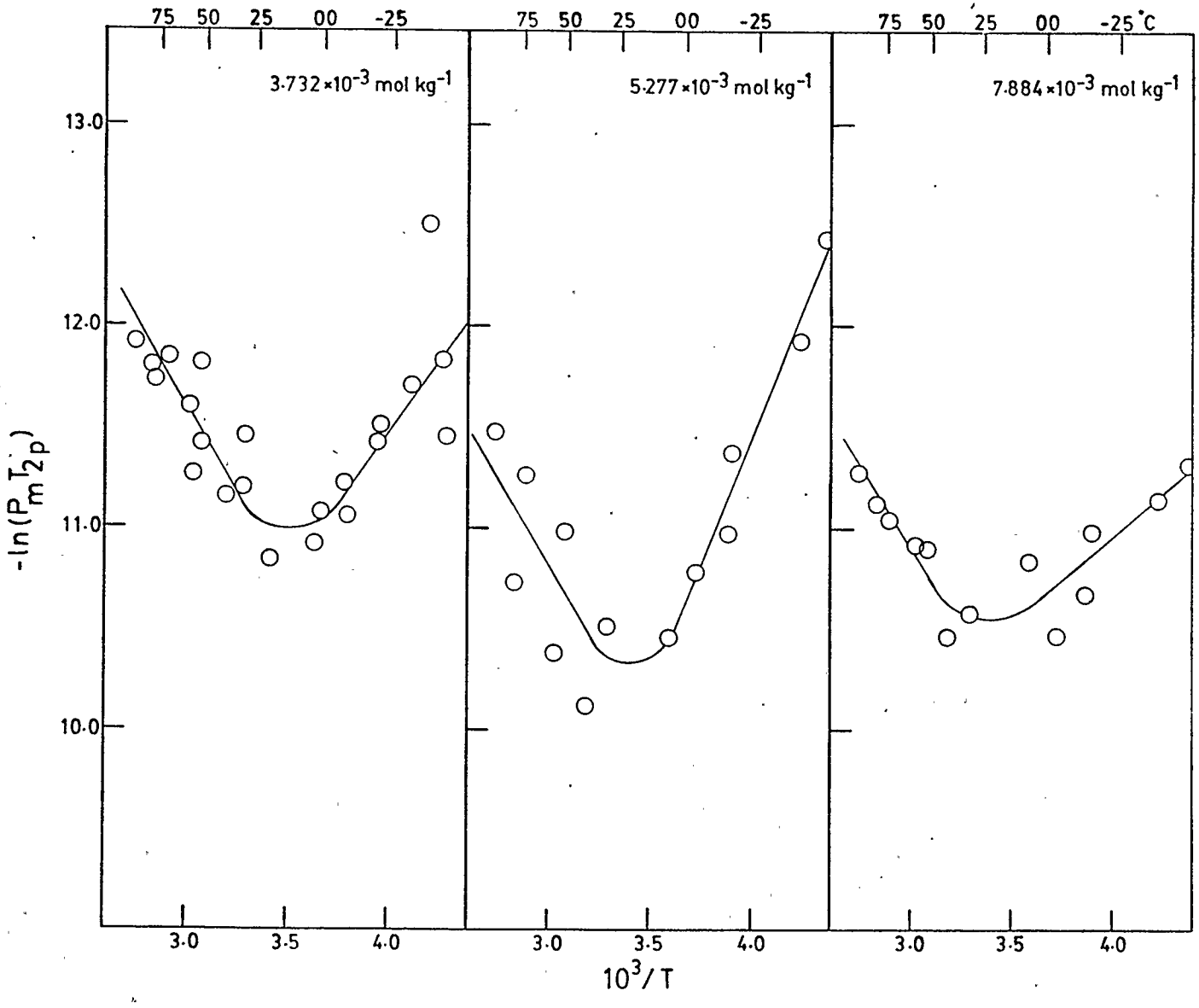
75 50 25 00 -25
75 50 25 00 -25
75 50 25 00 -25 °C
3·732×10⁻³ mol kg⁻¹
5·277×10⁻³ mol kg⁻¹
7·884×10⁻³ mol kg⁻¹
13·0
12·0
11·0
10·0
-ln(P_m T_2p)
3·0
3·5
4·0
10³/T

linewidth, on addition of $[Cu(Me_6tren)CH_3CN]^{2+}$, was rather small and its measurement error prone, consequently the data obtained are rather scattered. Furthermore, Figure [4-8] shows that outer-sphere contributions to the ^{14}N relaxation rate were significant. This means that the kinetic parameters for the exchange cannot be determined accurately, but it is evident that the rate of solvent exchange is at least 15 times slower than for the $[Cu(tren)CH_3CN]^{2+}$ ion in solution at 70 - 80°C.

The large error, the small range of temperatures (30 - 70°C) for the slow exchange process, and uncertainty about contributions from the outer sphere and possibly the fast exchange processes, would have made the results of a variable pressure study of this system unmeaningful.

4.4 Bisacetonitrile(1,4,8,11-tetraazacyclotetradecane)nickel(III) ion in Acetonitrile

An attempt was made to observe the ^{14}N relaxation of acetonitrile exchanging on $[Ni(cyclam)(CH_3CN)_2]X_3$, where X = ClO_4 and CF_3SO_3 (Figures [4-9], [4-10]). However, comparison with the ^{14}N relaxation in CH_3CN solutions containing only $[Ni(cyclam)](ClO_4)_2$ (Figure [4-11]) indicates that the major contribution to ^{14}N linebroadening in acetonitrile solutions of the nickel(III) complex is from the high spin form of the nickel(II) complex. Any nickel(III) complex surviving in these solutions is present as a minor component. Measurement of the UV-visible absorption spectra of the purported $[Ni(cyclam)(CH_3CN)_2]^{3+}$ solutions confirmed that at least 90% of the Ni(III) had been reduced to Ni(II) in the case of the perchlorate salt, and all of the nickel present had been reduced to Ni(II) in solutions of the triflate salt,

FIGURE [4-9]

Temperature dependence of $(P_m T_{2p})^{-1}$ for $[Ni(cyclam)](ClO_4)_2$, originally present as $[Ni(cyclam)(CH_3CN)_2](ClO_4)_3$, in CH_3CN

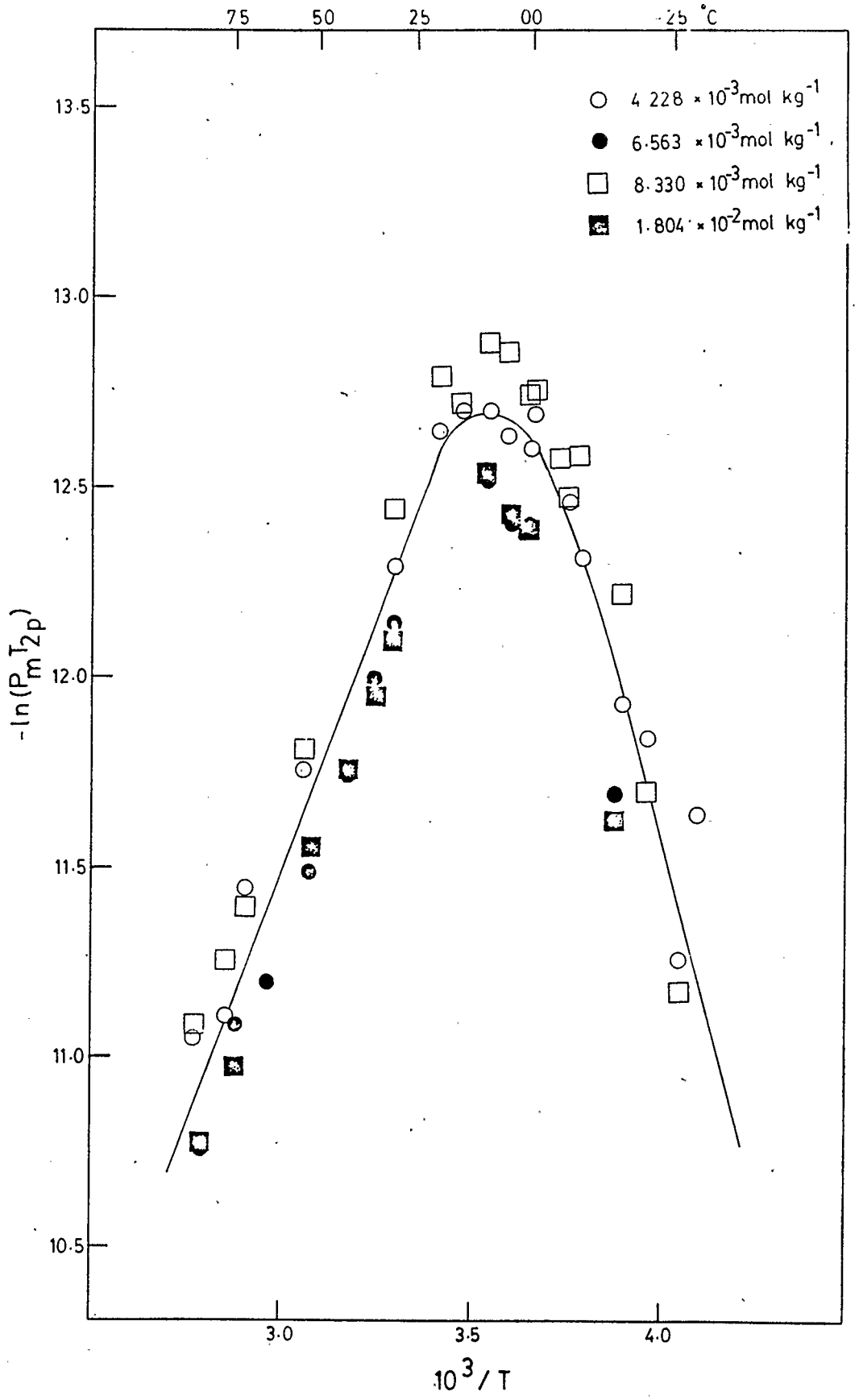
75
50
25
00
-25 °C
4 228 × 10⁻³mol kg⁻¹
6·563 ×10⁻³mol kg⁻¹
8·330 × 10⁻³mol kg⁻¹
1·804 × 10⁻²mol kg⁻¹
13·5
13·0
12·5
12·0
11·5
11·0
10·5
-ln(P_m T_2p)
3·0
3·5
4·0
10³ / T

FIGURE [4-10]

Temperature dependence of $(P_m T_{2p})^{-1}$ for $[Ni(cyclam)](CF_3SO_3)_2$, originally present as $[Ni(cyclam)(CH_3CN)_2](CF_3SO_3)_3$, in CH_3CN

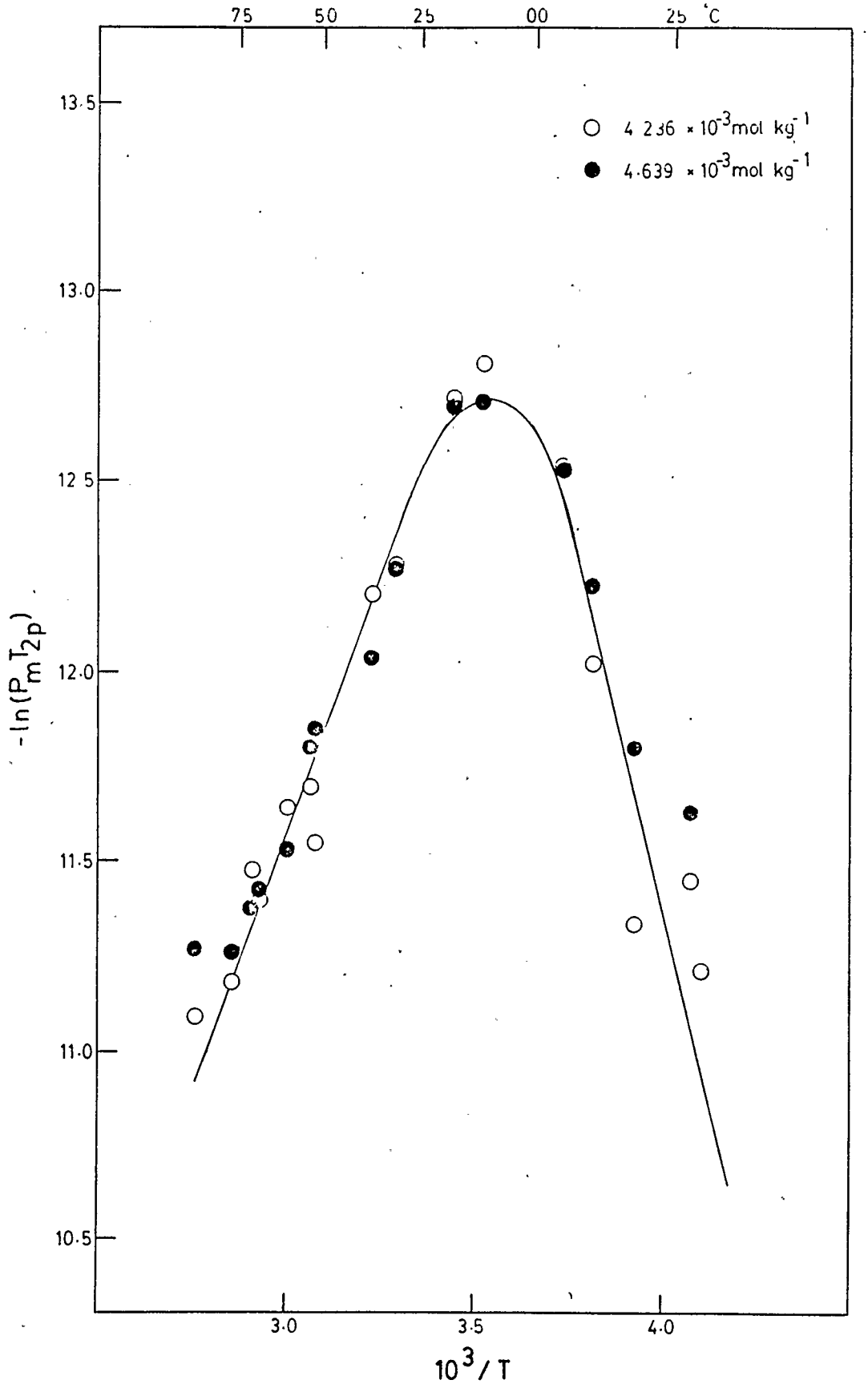
75
50
25
00
25 °C
13·5
13·0
12 5
12·0
11·5
11·0
10·5
○ 4 236 × 10⁻³mol kg⁻¹
● 4·639 × 10⁻³mol kg⁻¹
-ln(P_m T_2p)
3·0
3·5
4·0
10³ / T

FIGURE [4-11]

Temperature dependence of $(P_m T_{2p})^{-1}$ for

$[Ni(cyclam)](ClO_4)_2$ in CH_3CN

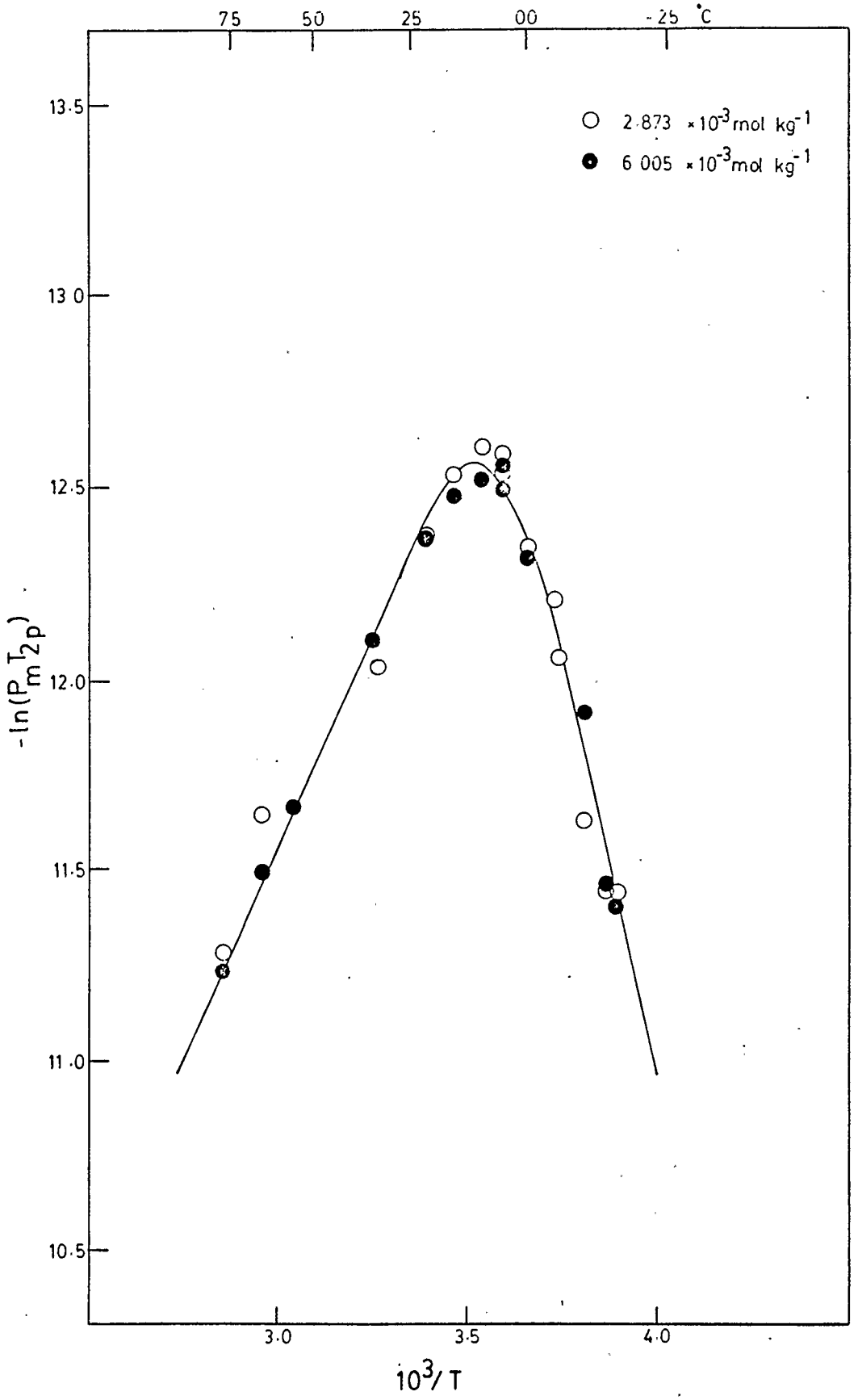
75
50
25
00
-25 °C
13·5
13·0
12·5
12·0
11·5
11·0
10·5
○ 2·873 ×10⁻³mol kg⁻¹
● 6 005 ×10⁻³mol kg⁻¹
-ln(P_m T_2p)
3·0
3·5
4·0
10³/T

during the course of these experiments. This could have occurred by reaction with some organic impurity in the acetonitrile solvent. Alternatively the triflate salt could have been reduced by removal of an acetonitrile molecule and subsequent coordination of $CF_3SO_3^-$ when the compound was pumped dry on a vacuum line.

The $[Ni(cyclam)]^{2+}$ contributes to the relaxation through the fast and slow exchange processes, independently of the concentration. The data obtained (Table [4-9]) were evaluated using the modified Swift-Connick expression [4-6] based on equations [2-9] and [2-10].

$$(P_m T_{2p})^{-1} = \Delta\omega^2_m \tau_m + \tau_m^{-1} \qquad [4\text{-}6]$$

Analysis over the temperature range 91.0 to -23.1°C gave the parameters: $\Delta H^* = 24.5 \pm 1.5$ kJ mol^{-1}, $\Delta S^* = -51.8 \pm 5.6$ J mol^{-1} K^{-1}, and $C = (163.3 \pm 9.3) \times 10^6$ rad K s^{-1}. This gives the rate constant at 25°C to be $k_{298} = 6.2 \times 10^5$ s^{-1}. A better fit was obtained when the data over the range 41.3 to -23.1°C was used, the parameters obtained were: $\Delta H^* = 34.6 \pm 1.3$ kJ mol^{-1}, $\Delta S^* = -14.0 \pm 5.0$ J mol^{-1} K^{-1} and $C = (167.6 \pm 4.5) \times 10^6$ rad K s^{-1}, giving $k_{298} = 9.9 \times 10^5$ s^{-1}.

Analysis of the data obtained with approximately 10% $[Ni(cyclam)(CH_3CN)_2](ClO_4)_3$ present (Table [4-10]), but calculating for 100% conversion to the nickel(II) complex, gave the parameters: $\Delta H^* = 21.1 \pm 1.3$ kJ mol^{-1}, $\Delta S^* = -60.4 \pm 4.6$ J K^{-1} mol^{-1}, $C = (167.0 \pm 7.9) \times 10^6$ rad K s^{-1}, $k_{298} = 8.7 \times 10^5$ s^{-1}, for the temperature range 91.0 to -23.1°C. For the temperature range 41.3 to -23.1°C the parameters obtained were: $\Delta H^* = 29.5 \pm 2.0$ kJ mol^{-1}, $\Delta S^* = -29.2 \pm 7.5$ J K^{-1} mol^{-1}, $C = (185.4 \pm 8.2) \times 10^6$ rad K s^{-1}, and $k_{298} = 1.2 \times 10^6$ s^{-1}.

TABLE [4-9]

Temperature dependence of $(P_m T_{2p})^{-1}$ for $[Ni(cyclam)](ClO_4)_2$ in CH_3CN

$10^3/T$ (K^{-1})	$-\ln(P_m T_{2p})$
2.873×10^{-3} mol kg^{-1}	
3.246	12.035
2.854	11.284
2.953	11.640
3.387	12.371
3.585	12.534
3.893	11.440
3.740	12.059
3.463	12.527
3.589	12.582
3.722	12.209
3.868	11.443
3.810	11.622
3.653	12.344
3.532	12.614
6.009×10^{-3} mol kg^{-1}	
3.246	12.107
3.036	11.658
2.854	11.238
2.953	11.489
3.387	12.366
3.585	12.544
3.893	11.403
3.462	12.472
3.589	12.485
3.868	11.462
3.810	11.911
3.653	12.317
3.532	12.516

TABLE [4-10]

Temperature dependence of $(P_m T_{2p})^{-1}$ for $[Ni(cyclam)(CH_3CN)_2](ClO_4)_2$, originally present as $[Ni(cyclam)(CH_3CN)_2](ClO_4)_3$, in CH_3CN

$10^3/T$ (K^{-1})	$-\ln(P_m T_{2p})$
4.228×10^{-3} mol kg^{-1}	
3.473	12.694
3.664	12.688
3.961	11.838
3.759	12.458
3.293	12.288
3.059	11.751
2.905	11.444
2.770	11.043
2.854	11.102
3.418	12.642
3.544	12.695
3.595	12.630
3.657	12.595
3.784	12.308
3.893	11.924
8.330×10^{-3} mol kg^{-1}	
3.473	12.713
3.664	12.752
3.961	11.692
3.759	12.470
3.293	12.435
3.059	11.808
2.905	11.392
2.770	11.084
2.854	11.252
3.418	12.789
3.544	12.875
3.595	12.856
3.657	12.742
3.784	12.583
3.893	12.213
3.728	12.570
6.563×10^{-3} mol kg^{-1}	
3.602	12.396
3.874	11.688
4.040	11.254
3.539	12.514
3.649	12.396
3.179	11.737
3.296	12.140
3.245	11.992
3.074	11.480
2.884	11.085
2.797	10.753
2.970	11.193
1.804×10^{-2} mol kg^{-1}	
3.602	12.421
3.874	11.618
4.040	11.171
3.539	12.530
3.649	12.399
3.179	11.746
3.296	12.092
3.245	11.949
3.074	11.547
2.854	10.969
2.797	10.763

Analysis of the data collected on the triflate salt solutions (Table [4-11]), again calculating for 100% Ni(II), for the temperature range 91.0 to -23.1°C gave the parameters: $\Delta H^* = 20.3 \pm 1.8$ kJ mol^{-1}, $\Delta S^* = -64.5 \pm 6.5$ J K^{-1} mol^{-1}, $C = (163.6 \pm 11.9) \times 10^6$ rad K s^{-1}, and $k_{298} = 7.3 \times 10^5$ s^{-1}. For the temperature range 41.2 to -23.1°C the triflate salt solutions, the parameters: $\Delta H^* = 33.2 \pm 2.8$ kJ mol^{-1}, $\Delta S^* = -15.8 \pm 10.4$ J K^{-1} mol^{-1}, $C = (207.3 \pm 14.5) \times 10^6$ rad K s^{-1}, and $k_{298} = 1.4 \times 10^6$ s^{-1}.

High pressure studies of the solutions containing [Ni(cyclam)-$(CH_3CN)_2$]$(ClO_4)_3$ (Table [4-12]) show that the rate constant is apparently a linear function of the pressure (Figure [4-12]). At these temperatures both the fast and slow exchange processes are significant and the pressure dependence of $-\ln(P_m T_{2p})$ should be nonlinear; ΔV^* values of +4.5 ± 0.4 at -17.5°C and +7 ± 3 at 26°C were computed from the pressure derivative of equation [4-6] with the assumption that the Curie constant, C, is independent of pressure. The volume of activation is presumably influenced by the volume change associated with the Ni(II) high spin - low spin equilibrium.

The diamagnetic analogue, $[Co(cyclam)(CH_3CN)_2]^{3+}$, of the nickel(III) complexes did not increase the ^{14}N linewidth of acetonitrile (Table [4-13]). The T_1 relaxation time (here, = T_2) is described by the linear expression [4-7], r = 0.9980 (Figure [4-13]).

$$\ln T_1 = -(2.562 \pm 0.053) - (895 \pm 15)/T \qquad [4\text{-}7]$$

Therefore the ^{14}N linebroadening of CH_3CN observed in the solutions of the Ni(cyclam) complexes was due entirely to the solvent exchange on the

TABLE [4-11]

Temperature dependence of $(P_m T_{2p})^{-1}$ for $[Ni(cyclam)(CH_3CN)_2](CF_3SO_3)_2$, originally present as $[Ni(cyclam)(CH_3CN)_2](CF_3SO_3)_3$, in CH_3CN

$10^3/T$ (K^{-1})	$-\ln(P_m T_{2p})$
4.236×10^{-3} mol kg^{-1}	
3.076	11.547
2.901	11.475
2.755	11.090
2.859	11.178
3.521	12.803
3.813	12.017
3.929	11.331
3.448	12.716
3.739	12.539
4.073	11.448
3.293	12.274
3.068	11.694
2.927	11.399
3.001	11.638
3.224	12.195
4.639×10^{-3} mol kg^{-1}	
3.076	11.846
2.901	11.372
2.755	11.262
2.859	11.257
3.521	12.706
3.813	12.213
3.929	11.796
3.445	12.693
3.739	12.539
4.073	11.627
3.293	12.271
3.068	11.797
2.927	11.422
3.004	11.530
3.228	12.029

TABLE [4-12]

Pressure dependence of $(P_m T_{2p})^{-1}$ for $[Ni(cyclam)(CH_3CN)_2](ClO_4)_2$, originally present as $[Ni(cyclam)(CH_3CN)_2](ClO_4)_3$, in CH_3CN

P(MPa)	$-\ln(P_m T_{2p})$
301.89 K, 4.795×10^{-3} mol kg^{-1}	
82.9	12.440
162.0	12.483
201.0	12.658
119.1	12.493
40.8	12.411
1.8	12.391
0.1	12.269
61.5	12.396
139.9	12.557
200.6	12.636
179.7	12.354
99.9	12.529
19.5	12.362
1.8	12.340
82.5	12.494
160.5	12.614
259.27 K, 1.024×10^{-2} mol kg^{-1}	
0.1	12.034
81.5	12.076
159.0	11.648
40.2	11.973
5.3	11.986
102.8	11.940
191.7	11.769
145.9	12.250
51.2	11.956
2.3	12.095
301.30 K, 1.024×10^{-2} mol kg^{-1}	
0.1	12.221
84.9	12.233
162.1	12.562
200.7	12.468
120.6	12.320
39.9	12.186
1.8	12.109
50.9	12.281
191.0	12.342
101.2	12.384

FIGURE [4-12]

Pressure dependence of $(P_m T_{2p})^{-1}$ for $[Ni(cyclam)](ClO_4)_2$, originally present as $[Ni(cyclam)(CH_3CN)_2](ClO_4)_3$, in CH_3CN

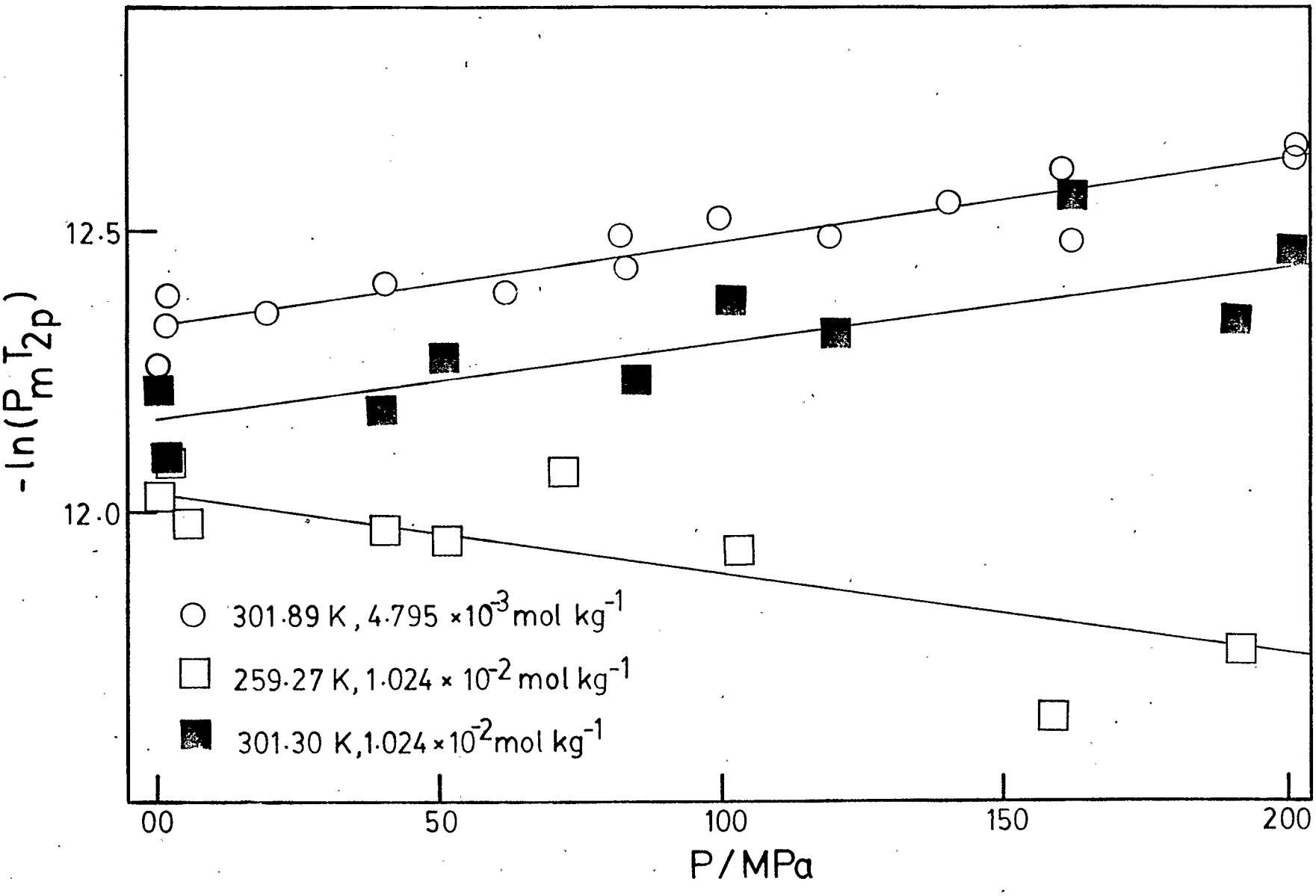
12·5
12·0
$-\ln(P_m T_{2p})$
○ 301·89 K, 4·795 ×10⁻³ mol kg⁻¹
□ 259·27 K, 1·024 × 10⁻² mol kg⁻¹
■ 301·30 K, 1·024 × 10⁻² mol kg⁻¹
00
50
100
150
200
P/MPa

TABLE [4-13]

Temperature dependence of the ^{14}N longitudinal relaxation time T_1 (= T_2) for 1.310×10^{-2} mol kg^{-1} $[Co(cyclam)(CH_3CN)_2](ClO_4)_3$ in CH_3CN

$10^3/T$ (K^{-1})	$-\ln T_1$
3.444	-5.638
3.736	-5.913
4.073	-6.200
4.262	-6.421
3.294	-5.501
3.074	-5.317
2.928	-5.222
3.004	-5.263
3.225	-5.458

FIGURE [4-13]

Temperature dependence of the ^{14}N longitudinal relaxation T_1 (= T_2) for 1.310×10^{-2} mol kg^{-1} $[Co(cyclam)(CH_3CN)_2](ClO_4)_3$ in CH_3CN

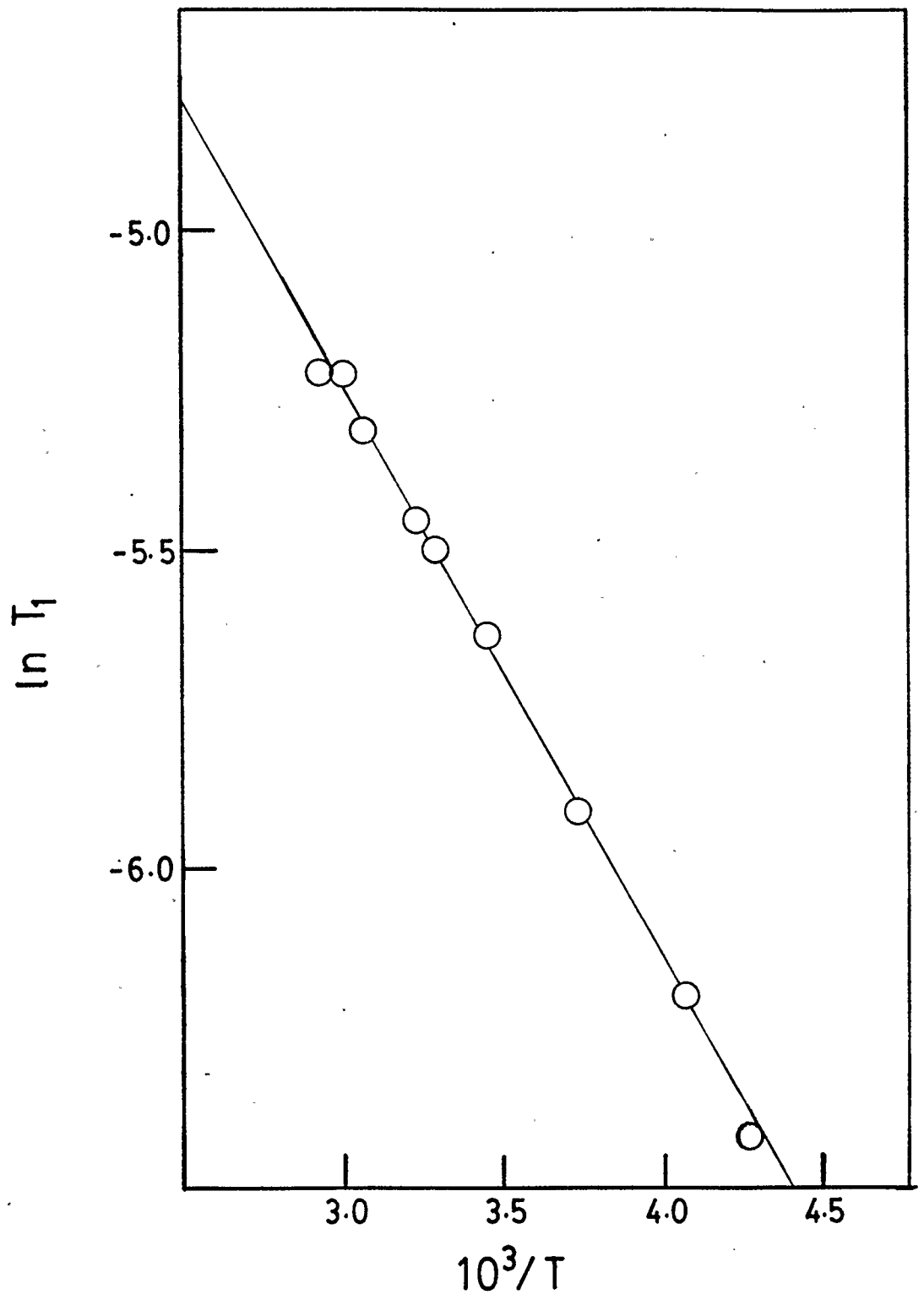
-5.0
-5.5
-6.0
ln T1
3.0
3.5
4.0
4.5
10³/T

paramagnetic Ni(II) centre, rather than to an effect of the cyclam complexes on the viscosity of the medium.

Chapter 5 Interpretation of Results

5.1 Acetonitriletris(2-aminoethyl)aminecopper(II) and acetonitriletris(N,N',N"-dimethyl-2-aminoethyl)aminecopper(II) Perchlorate in Acetonitrile

The exchange of solvent on the $[CuL(CH_3CN)]^{2+}$ ion, L = tren and Me_6tren, (equation [5-1]) can be described

$$[CuL(CH_3CN)]^{2+} + (CH_3CN)^{o} \rightleftharpoons [CuL(CH_3CN)(CH_3CN)^{o}]^{2+}$$

$$\Downarrow$$

$$[CuL(CH_3CN)^{o}]^{2+} + CH_3CN \qquad [5\text{-}1]$$

by the rate expression [5-2] where the rate constant, k_{ex}, is equivalent to $(P_mT_{2p})^{-1}$ in the slow exchange region.

$$R = k_{ex}[[CuL(CH_3CN)]^{2+}] \qquad [5\text{-}2]$$

However, from the experimental data (Section 4.2, 4.3) it can be seen that $(P_mT_{2p})^{-1}$ is dependent on the concentration of the copper complex and perchlorate ion. This suggests that another reaction, such as ion-pairing (equation [5-3a]) or complex formation (equation [5-3b]), is interfering with the solvent exchange.

$$[CuL(CH_3CN)]^{2+} + ClO_4^- \overset{K_c}{\rightleftharpoons} [CuL(CH_3CN)]^{2+}(ClO_4)^- \qquad [5\text{-}3a]$$

$$\rightleftharpoons [CuL(ClO_4)]^{+} + CH_3CN \qquad [5\text{-}3b]$$

In the first case, the ClO_4^- ion is in the second solvation sphere and hinders the exchange of CH_3CN between the first solvation sphere and the bulk solvent.[82] In the second instance, the ClO_4^- ion has displaced the CH_3CN from the first solvation sphere, therefore removing it from the paramagnetic centre and preventing direct relaxation by Cu(II). The possible formation of ion-pairs for the Me_6tren complex has been discussed previously.[60]

The amount of copper complex ion-paired in solution is given by equation [5-4], where $[[CuL(CH_3CN)]^{2+}]_o$ is the total amount of the complex in solution, and $[[CuL(CH_3CN)]^{2+}]$ is the amount of complex available for solvent exchange.

$$[[CuL(CH_3CN)]^{2+}(ClO_4)^-] = [[CuL(CH_3CN)]^{2+}]_o - [[CuL(CH_3CN)]^{2+}] \quad [5\text{-}4]$$

The equilibrium constant, K_c, can be described by expression [5-5]:

$$K_c = \frac{[[CuL(CH_3CN)]^{2+}(ClO_4)]^-}{[[CuL(CH_3CN)]^{2+}][ClO_4^-]} = \frac{[[CuL(CH_3CN)]^{2+}]_o - [[CuL(CH_3CN)]^{2+}]}{[[CuL[(CH_3CN)]^{2+}][ClO_4^-]} \quad [5\text{-}5]$$

Rearrangement of this equation gives

$$[[CuL(CH_3CN)]^{2+}] = \frac{[[CuL(CH_3CN)]^{2+}]_o}{1 + K_c[ClO_4^-]} \quad [5\text{-}6]$$

Substitution into equation [5-2] gives the rate expression [5-7],

$$R = k_{ex} \frac{[[CuL(CH_3CN)]^{2+}]_o}{1 + K_c[ClO_4^-]} \qquad [5\text{-}7]$$

with an observed rate constant, k_o, defined by equation [5-8].

$$k_o = \frac{k_{ex}}{1 + K_c[ClO_4^-]} \qquad [5\text{-}8]$$

Therefore, the dependence of k_o on $[ClO_4^-]$ (Table [5-1]) can be used to find K_c and k_{ex}. This treatment assumes that: 1) the perchlorate complex (or ion-pair) does not exchange CH_3CN at all, which is certainly the case for inner sphere complexing (equation [5-3b]), although UV-vis spectra did not show evidence of this type of complex; and 2) the activity coefficients are unity or otherwise not taken into account.

The $[ClO_4^-]$ dependence of k_o at 298 and 313 K is shown in Figure [5-1]. For 298 K the straight line ($r = 0.9692$) gives 1.33×10^6 s^{-1} and 218 kg mol^{-1} for k_{ex} and K_c respectively, and at 313 K the corresponding values ($r = 0.9776$) are 2.98×10^6 s^{-1} and 320 kg mol^{-1}. These give the enthalpy of activation, $\Delta H^* = 39$ kJ mol^{-1}, and for the equilibrium [5-3], $\Delta H_c = 19.9$ kJ mol^{-1}.

Unfortunately, insufficient variable pressure data were obtained so definite values for the volumes of activation, ΔV^*, and ion pair formation, ΔV_c, could not be determined. The dependence of k_o on pressure at low pressures is probably dominated by the breaking up of ion-pairs, and gives $(-\Delta V_c + \Delta V^*) \simeq -30$ cm^3 mol^{-1}. As the pressure is increased, the free ion $Cu(tren)CH_3CN^{2+}$ becomes predominant giving $\Delta V^* \approx -2$ cm^3 mol^{-1}. However, to ensure that a limiting slope corresponding to ΔV^* has been obtained the exchange reaction would have to be studied at higher pressures.

TABLE [5-1]

Dependence of k_0 on $[ClO_4^-]$

$[[Cu(tren)CH_3CN]^{2+}]$ x 10^3 mol kg^{-1}	$[NaClO_4]$ x 10^3 mol kg^{-1}	$[ClO_4]^-$ x 10^3 mol kg^{-1}	$k_0(298)$ x 10^{-6} s^{-1}	$k_0(313)$ x 10^{-6} s^{-1}	$1/k_0(298)$ x 10^6 s	$1/k_0(313)$ x 10^6 s
1.05	0	2.10	~0.67	~1.21	1.50	0.823
	4.93	7.03	0.568	1.04	1.76	0.966
1.18	0	2.36	0.684	1.24	1.46	0.807
	4.73	7.09	0.504	0.937	1.98	1.07
	9.46	11.82	0.36	0.660	2.78	1.52
2.02	0	4.04	1.02	1.71	0.98	0.586
6.55	0	13.11	0.425	0.667	2.35	1.50
13.78	0	27.56	0.181	0.285	5.52	3.47

FIGURE [5-1]

Dependence of the observed rate constant, k_o,

on perchlorate ion concentration

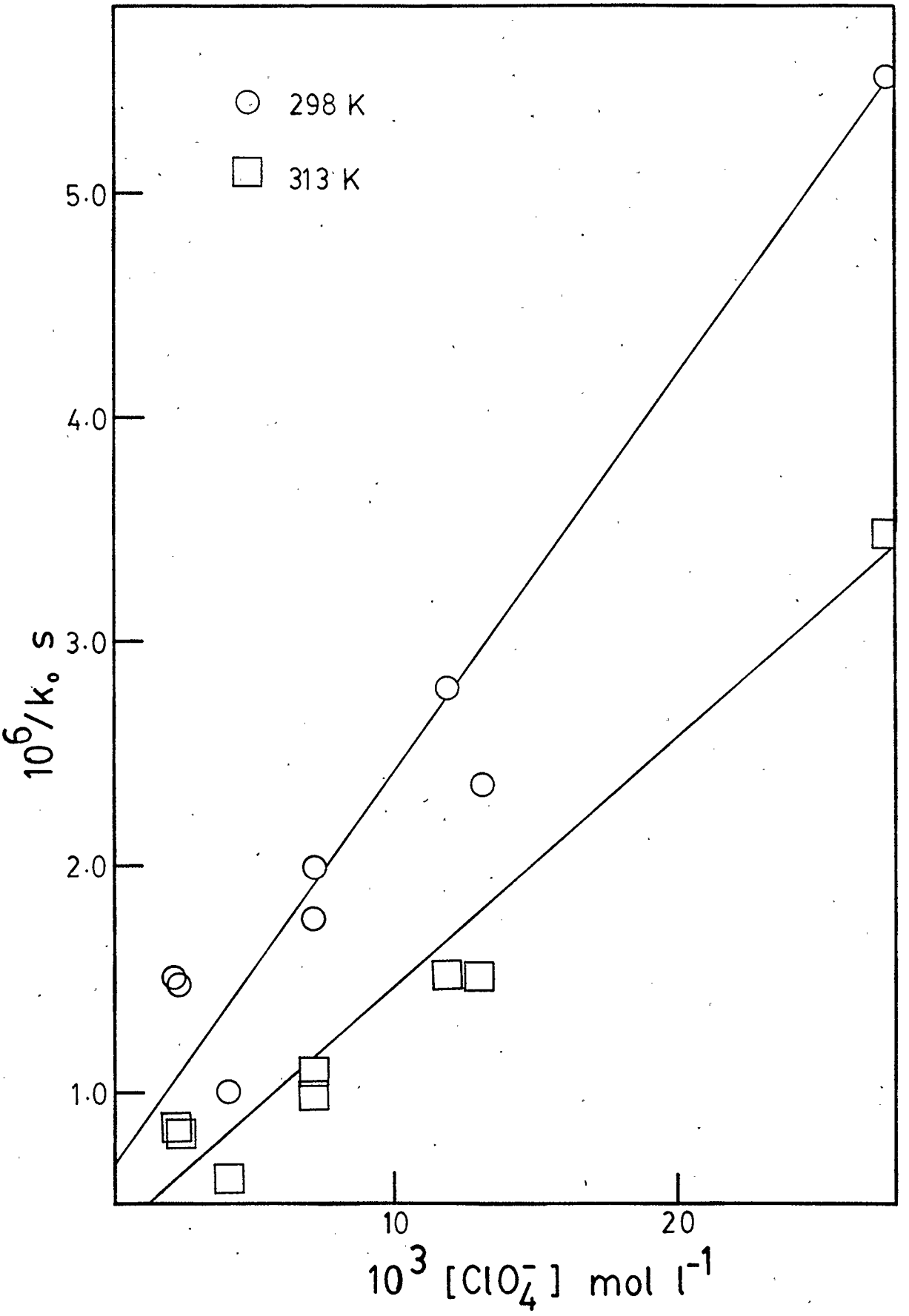
298 K
313 K
5.0
4.0
3.0
2.0
1.0
$10^6/k_o$ s
10
20
10^3 [ClO_4^-] mol l^{-1}

In a previous study[49] of CH_3CN solvent exchange on $[Cu(tren)CH_3CN]^{2+}$ and $[Cu(Me_6tren)CH_3CN]^{2+}$, the dependence of k_o on the anion concentration was not considered. The rate constants reported were $k_{298} = (5.1 \pm 0.7) \times 10^3\ s^{-1}$ and $k_{228} < 10^2$ for $[Cu(tren)CH_3CN]^{2+}$ and $[Cu(Me_6tren)CH_3CN]^{2+}$ respectively.

It has been previously observed[49,61,62] that the rate of solvent exchange on the copper-tren complex is much slower than on the hexasolvated copper(II) ion. For cobalt(II) and nickel(II), however, the coordination of the quadridentate tren ligand results in a rate of solvent exchange that is faster than for the hexasolvated ion. It has been suggested[49,61,62] that the rapid exchange on the hexasolvated copper(II) ion is due to a rate determining exchange between the bulk solvent and the axial position, followed by a Jahn-Teller inversion that interchanges the axial and equatorial positions. Coordination of the tren ligand forms a trigonal bipyramidal complex that prevents the inversion step, and thus causes a slower rate of exchange. While the value of k_{298} for CH_3CN exchange on $[Cu(tren)CH_3CN]^{2+}$ reported here is several orders of magnitude greater than previously found,[49] it is still much less than the value for acetonitrile exchange on hexakis-acetonitrile-copper(II) ion, $k_{298} \gg 3.7 \times 10^8\ s^{-1}$.[26]

These studies suggest that an associative interchange mechanism, I_a, is followed for acetonitrile exchange on the tren and Me_6tren complexes of copper(II). The large negative values obtained for ΔS^* for all solutions, and the negative, although unreliable, values for ΔV^* support this. Further evidence for this type of exchange mechanism comes from the lower rate of exchange observed when the hydrogen atoms on the tren ligand are replaced with the methyl groups of

Me_6tren, which would present increased steric hindrance to associative attack but would presumably accelerate a dissociative process through steric decompression.

5.2 Bisacetonitrile(1,4,8,11-tetraazacyclotetradecane)nickel(III) ion in Acetonitrile

The experimental results (Section 4.4) suggest that the nickel(III) complex was a minor component of the solutions studied and that the $CH_3C^{14}N$-NMR line broadening observed was due to acetonitrile exchange on the high spin bisacetonitrile(1,4,8,11,tetraazacyclotetradecane)-nickel(II) ion. This complex is in equilibrium (equation [5-9]) with the low spin $[Ni(cyclam)]^{2+}$ ion and therefore the amount present in solution will be temperature dependent.

$$[Ni(cyclam)(CH_3CN)_2]^{2+} \underset{}{\overset{K_{eq}}{\rightleftharpoons}} [Ni(cyclam)]^{2+} + 2CH_3CN \qquad [5\text{-}9]$$

The equilibrium constant, K_{eq}, is given by equation [5-10], where $[[NiL]^{2+}]_o$ is the total amount of nickel in solution and $[[NiL(CH_3CN)_2]^{2+}]$ is the amount of the high spin complex present.

$$K_{eq} = \frac{[[NiL]^{2+}]}{[[NiL(CH_3CN)_2]^{2+}} = \frac{[[NiL]^{2+}]_o - [[NiL(CH_3CN)_2]^{2+}]}{[[NiL(CH_3CN)_2]^{2+}]} \qquad [5\text{-}10]$$

Rearrangement of equation [5-10] gives:

$$[[NiL(CH_3CN)_2]^{2+}] = \frac{K_{eq}[[NiL]^{2+}]_o}{1 + K_{eq}} \qquad [5\text{-}11]$$

The rate of exchange is given by equation [5-12]:

$$R = 2k_{ex}[[NiL(CH_3CN)_2]^{2+}] \qquad [5\text{-}12]$$

Substitution of equation [5-11] gives the rate of exchange as a function of the total nickel(II) concentration (equation [5-13]) with an observed rate constant given by equation [5-14].

$$R = \frac{2k_{ex}\ K_{eq}}{1 + K_{eq}}\ [[NiL]^{2+}]_o \qquad [5\text{-}13]$$

$$k_o = \frac{k_{ex}\ K_{eq}}{1 + K_{eq}} \qquad [5\text{-}14]$$

The equilibrium between the high spin and low spin Ni(II) complexes has been studied in water,[70] where it was found that $[[NiL]^{2+}]$ increased with temperature and upon addition of the inert electrolyte, $NaClO_4$. The equilibrium constant, K_{eq}, can be found using equation [5-15], where ε_o is the molar absorbance of the low spin complex and A is the absorbance of the low spin Ni(II) complex.

$$K_{eq} = \frac{A}{[[NiL]^{2+}]^o_o\ \varepsilon_o b - A} \qquad [5\text{-}15]$$

$[[NiL]^{2+}]^o_o$ is the total concentration of nickel present, corrected for density changes with temperature, and b is the pathlength of the cell.

A solution of 5.110×10^{-3} mol L^{-1} $[Ni(cyclam)](ClO_4)_2$ and 0.4759 mol L^{-1} $NaClO_4$ in CH_3CN gave a molar absorbance ε_o = 22.66 L mol^{-1} cm^{-1}

and showed no further increase with temperature. The temperature dependence of K_{eq} (Table [5-2]) is shown in Figure [5-2], where the straight line ($r = 0.9578$) is described by equation [5-16]. The enthalpy of the equilibrium is therefore $\Delta H_{eq} = 19.9 \pm 2.7$ kJ mol^{-1}.

$$\ln K_{eq} = (8.56 \pm 1.1) - (2.39 \pm 0.32) \times 10^3/T \qquad [5\text{-}16]$$

The value of K_{eq} at 25°C is 1.7, thus suggesting that 36.6% of the nickel(II) complex present is in the high spin form.

Calculation of k_{ex} using equations [5-14] and [5-15] (Table [5-3]) gave the following parameters for CH_3CN exchange on the high spin nickel(II) complex: $\Delta H^* = 32.1 \pm 0.4$ kJ mol^{-1}, $\Delta S^* = 76.2 \pm 0.4$ J K^{-1} mol^{-1}, and $k_{298} = 1.58 \times 10^6$ s^{-1}. The parameters reported by Hunt[70] for water exchange on the high spin $[Ni(cyclam)(H_2O)_2]^{2+}$ complex were: $\Delta H^* = 37.7$ kJ mol^{-1}, $\Delta S^* = 29.3$ J K^{-1} mol^{-1} and $k_{298} = 2 \times 10^7$ s^{-1}. The value of K_{eq} reported for the high spin - low spin equilibrium was 2.3 ± 1.

The rapid rate of CH_3CN exchange on $[Ni(cyclam)(CH_3CN)_2]^{2+}$ suggests that determination of activation parameters for the nickel(III) complex would be difficult since even a small amount of nickel(II) would have a large affect on the measured $(P_m T_{2p})^{-1}$ values. Also, electron exchange between the Ni(II)- and Ni(III)-cyclam could influence the observed rate of exchange; the rate constant for electron exchange between $Ni(II)(cyclam)^{2+}$ and $Ni(III)(cyclam)^{3+}$ in water has been reported as being approximately 10^3 l mol^{-1} s^{-1}.[83]

The large positive entropy of activation suggests that the solvent exchange on $[Ni(cyclam)(CH_3CN)_2]^{2+}$ follows a dissociative interchange,

TABLE [5-2]

Temperature dependence of K_{eq} for 4.669×10^{-3} mol l^{-1} $[Ni(cyclam)]^{2+}$ in CH_3CN

$10^3/T$ (K^{-1})	ln K_{eq}
3.341	0.3715
3.227	0.880
3.156	1.083
3.271	0.7053
3.462	0.3235
3.515	0.1969
3.405	0.4558

FIGURE [5-2]

Temperature dependence of K_{eq} for

4.669×10^{-3} mol l^{-1} $[Ni(cyclam)]^{2+}$ in CH_3CN

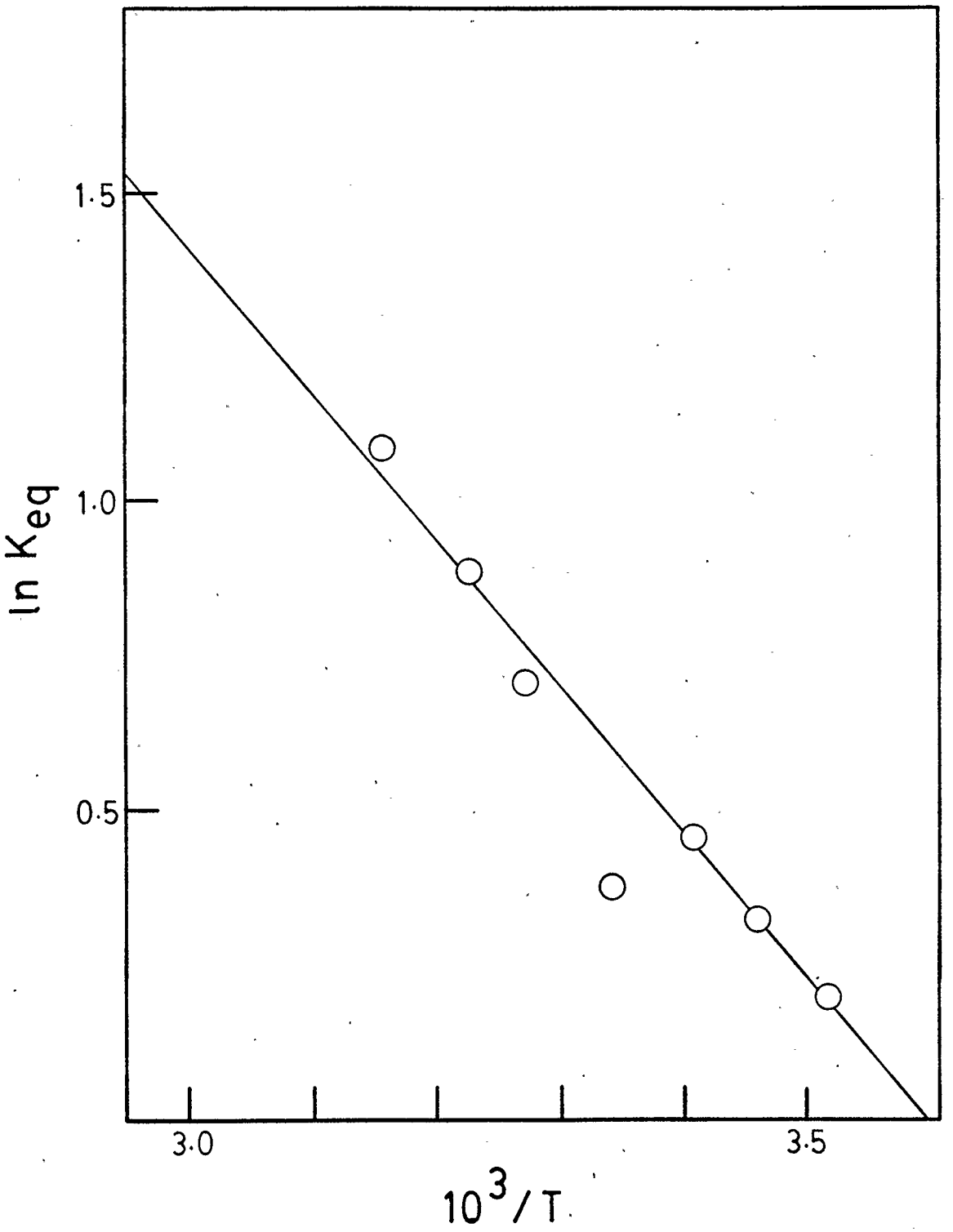
1·5
1·0
0·5
ln K_{eq}
3·0
3·5
$10^3 / T$

TABLE [5-3]

Temperature dependence of k_{ex} for CH_3CN exchange on $[Ni(cyclam)(CH_3CN)_2]^{2+}$

$10^3/T$ (K^{-1})	$k_{obs}(10^{-6})$	k_{eq}	$k_{ex}(10^{-6})$
3.532	0.453	1.121	0.857
3.411	0.775	1.445	1.29
3.354	1.00	1.714	1.58
3.299	1.28	1.957	1.93
3.193	2.05	2.517	2.86

I_d, type mechanism. This is supported by previous studies of CH_3CN exchange on the Me_4cyclam-Ni(II) complex.[40]

CHAPTER 6 CONCLUSIONS

The results reported in this work indicate that while the Swift-Connick theory can be used to obtain solvent exchange parameters from NMR linewidths, the experiment can be sensitive to anion-cation pairing or complexing especially in solvents of low dielectric constant such as acetonitrile, and, where the amount of paramagnetic solute is relatively low, to oxidation or reduction of the solute of interest by trace impurities.

Further investigations of the CH_3CN exchange on $[Cu(tren)CH_3CN](ClO_4)_2$ are required to obtain accurate values of the volume of activation, ΔV^*, and the volume change on ion-pair formation, ΔV_c. Of particular importance are experiments using a larger pressure range with variable perchlorate concentration. In order to study the solvent exchange on the Cu-tren and -Me_6tren complexes without interference from the ion-pairing reaction, ClO_4^- should be replaced by another anion that has little or no tendency to coordinate. An alternative is to use a solvent with a larger dielectric constant. The relatively slow rate of exchange on these copper complexes is of interest as there is a similarity with exchange on some copper containing enzymes.[62,63,84] This suggests that the mechanism of exchange at the copper sites of the enzyme is also associative.[61]

The stability of the Ni(III) complex in water has been increased by the addition of $HClO_4$ to the solution and by adding SO_4^{2-} to coordinate to one of the axial positions.[65,81] The main problem is to ensure that 100% of the nickel is present as the Ni(III) complex. Of further interest would be the study of solvent exchange on complexes of quinquedentate macrocyclic ligands[85,86] where only one exchange site is

available. The importance of macrocyclic complexes as models for biological systems has been discussed previously[67] and octahedral Ni(III) centres have been observed in natural systems.[87]

REFERENCES

1. Gutowsky, H.S. and Saika, A. J. Chem. Phys. 21, 1688 (1953).
2. Gutowsky, H.S. and Holm, C.H. J. Chem. Phys. 25, 1228 (1956).
3. Lincoln, S.F. Progress in Reaction Kinetics 9, 1 (1977).
4. Moniz, W.B. and Dixon, J.A. J. Am. Chem. Soc. 83, 1671 (1961); Jensen, F.R. et al. J. Am. Chem. Soc. 84, 386 (1962).
5. Phillips, W.D. J. Chem. Phys. 23, 1363 (1955); Gutowsky, H.S. and Holm, C.H. J. Chem. Phys. 25, 1228 (1956).
6. Stranks, D.R. Pure Appl. Chem. 38, 303 (1974).
7. Stranks, D.R. and Lawrence, G.A. Acc. Chem. Res. 12, 403 (1979).
8. Palmer, D.A. and Kelm, H. Coord. Chem. Rev. 36, 89 (1981).
9. Asano, T. and LeNoble, W.J. Chem. Revs. 78, 407 (1978).
10. Swaddle, T.W. Inorg. Chem. 22, 2663 (1983).
11. Jonas, J. Adv. Magn. Reson. 6, 73 (1963).
12. Jonas, J. Annu. Rev. Phys. Chem. 26, 167 (1975).
13. Jonas, J. "High Pressure Chemistry", N.A.T.O. Advanced Study Institute 41, 65 (1978).
14. Jonas, J. Rev. Phys. Chem. Jpn. 50, 126 (1980).
15. Jonas, J. Science 216, 1179 (1982).
16. Swift, T.J. and Connick, R.E. J. Chem. Phys. 37, 307 (1962).
17. Swift, T.J. and Connick, R.E. J. Chem. Phys. 41, 2553 (1964).
18. Langford, C.H. and Gray, H.B. "Ligand Substitution Processes" (1965), Benjamin Inc.
19. Amman, C.; Moore, P.; and Merbach, A.E. Helv. Chim. Acta. 63, 268 (1980).
20. Angerman, N.S. and Jordan, R.B. Inorg. Chem. 8, 65 (1969).

21. Watkins, C.L.; Vigee, G.S.; and Harris, M.E. J. Phys. Chem. 77, 855 (1973).

22. Grant, M.W.; Dodgen, H.W.; and Hunt, J.P. Inorg. Chem. 10, 71 (1971).

23. Goldammer, E.V. and Bassaris, Ch. J. Soln. Chem. 9, 237 (1980).

24. Sisley, M.J.; Yano, Y.; and Swaddle, T.W. Inorg. Chem. 21, 1141 (1982).

25. Purcell, W.L. and Marianelli, R.S. Inorg. Chem. 9, 1724 (1970).

26. Vigee, G.S.; Watkins, C.L.; and Harris, M.E. J. Inorg. Nucl. Chem. 42, 1441 (1980).

27. Zetter, M.S.; Grant, M.W.; Wood, E.J.; Dodgen, H.W.; and Hunt, J.P. Inorg. Chem. 11, 2701 (1972).

28. Breivogel, F.W. J. Phys. Chem. 73, 4203 (1969).

29. Hodgkinson, J. and Jordan, R.B. J. Am. Chem. Soc. 95, 763 (1973).

30. Meyer, F.K.; Monnerat, A.; Newman, K.E.; and Merbach, A.E. Inorg. Chem. 21, 774 (1982).

31. West, R.J. and Lincoln, S.F. Inorg. Chem. 11, 1688 (1972).

32. Kapur, V.K. and Wayland, B.B. J. Phys. Chem. 77, 634 (1973).

33. Matwiyoff, N.A and Hooker, S.V. Inorg. Chem. 6, 1127 (1967).

34. Monnerat, A.; Moore, P.; Newman, K.; and Merbach, A.E. Inorg. Chim. Acta 47, 139 (1981).

35. Meyer, F.K.; Newman, K.E.; and Merbach, A.E. Inorg. Chem. 18, 2142 (1979).

36. Yano, Y.; Fairhurst, M.T.; and Swaddle, T.W. Inorg. Chem. 19, 3267 (1980).

37. Boubel, J.C.; Delpuech, Jean J.; and Peguy, A.A. Chem. and Biol. Appl. Relax. Spectro. 323 (1975), Wyn-Jones (ed.).

38. West, R.J. and Lincoln, S.F. Inorg. Chem. 12, 494 (1973).

39. West, R.J. and Lincoln, S.F. Aust. J. Chem. 27, 97 (1974).

40. Helm, L.; Meier, P.; Merbach, A.E.; and Tregloan, P.A. Inorg. Chim. Acta 73, 1 (1983).

41. Desai, A.G.; Dodgen, H.W.; and Hunt, J.P. J. Am. Chem. Soc. 91, 5001 (1969).

42. Ducommun, Y.; Earl, W.L.; and Merbach, A.E. Inorg. Chem. 18, 2754 (1979).

43. Lincoln, S.F. and West, R.J. Aust. J. Chem. 26, 255 (1973).

44. Newman, K.E.; Meyer, F.K.; and Merbach, A.E. J. Am. Chem. Soc. 101, 1470 (1979).

45. Batstone-Cunningham, R.L.; Dodgen, H.W.; and Hunt, J.P. Inorg. Chem. 21, 3831 (1982).

46. Lincoln, S.F. and West, R.J. J. Am. Chem. Soc. 96, 400 (1974).

47. Rablen, D.; Dodgen, H.; Hunt, J.P. J. Am. Chem. Soc. 94, 1771 (1972).

48. Earl, W.L.; Meyer, F.K.; and Merbach, A.E. Inorg. Chim. Acta 25, L91 (1977).

49. West, R.J. and Lincoln, S.F. J. Chem. Soc. Dalton, 281 (1974).

50. Merbach, A.E. and Vanni, H. Helv. Chim. Acta 60, 1124 (1977).

51. Poupko, R. and Luz. Z. J. Chem. Phys. 57, 3311 (1972).

52. Mann, B.E. Annu. Rep. on NMR Spec. 12, 263 (1982); Nuclear Magnetic Resonance 1, 238 (1972); **ibid** 5, 134 (1976).

53. Ducommun, Y.; Earl, W.L.; and Merbach, A.E. Inorg. Chem. 18, 2142 (1979).

54. Krug, R.R.; Hunter, W.G.; and Grieger, R.A. Nature 261, 566 (1976); J. Phys. Chem. 80, 2335 (1976); **ibid** 80, 2341 (1976).

55. Merbach, A.E. Pure Appl. Chem. 54, 1479 (1982).

56. Jain, P.C. and Lingafelter, E.C. J. Am. Chem. Soc. 89, 724 (1967).

57. Di Vaira, M. and Orioli, P.L. Acta Cryst. B24, 595 (1968).

58. Cristini, A. and Ponticelli, G. Inorg. Nucl. Chem. 34, 2691 (1973).

59. Massacessi, M. and Ponticelli, G. Gazz. Chim. Ital. 104, 789 (1974).

60. Ciampolini, M. and Nardi, N. Inorg. Chem. 5, 41 (1966).

61. Cayley, G.R.; Kelly, I.D.; Knowles, P.F.; and Yadav, K.D.S. J. Chem. Soc. Dalton, 2370 (1981).

62. Cayley, G.R.; Cross, D.; and Knowles, P. J. Chem. Soc. Chem. Commun. 837 (1976).

63. Coates, J.H.; Collins, P.R.; and Lincoln, S.F. J. Chem. Soc. Faraday I 75, 1236 (1979).

64. Lincoln, S.F.; Coates, J.H.; Dodderidge, B.G.; Hounslow, A.M.; and Pisanello, D.L. Inorg. Chem. 22, 2869 (1983).

65. Haines, R.I. and McAuley, A. Coord. Chem. Revs. 39, 77 (1981).

66. Melson, G.A. (Editor) "Coordination Chemistry of Macrocyclic Compounds", Plenum Press (1979).

67. Busch, D.H. Acc. Chem. Res. 11, 392 (1978).

68. Nag, K. and Chakravorty, A. Coord. Chem. Revs. 33, 87 (1980).

69. Haines, R.I. and McAuley, A. Inorg. Chem. 19, 719 (1980).

70. Pell, R.J.; Dodgen, H.W.; and Hunt, J.P. Inorg. Chem. 22, 529 (1983).

71. Herron, N. and Moore, P. J. Chem. Soc. Dalton, 442 (1979).

72. Curzon, E.H.; Herron, N.; and Moore, P. J. Chem. Soc. Dalton 574 (1980).

73. Bull, T.F. and Jonas, J. J. Chem. Phys. 53, 3315 (1970).

74. Moniz, B. and Gutowsky, H.S. J. Chem. Phys. 38, 1155 (1963).

75. Bopp, T.T. J. Chem. Phys. 24, 1169 (1971).

76. Swaddle, T.W. Coord. Chem. Rev. 14, 217 (1974).

77. Vanni, H.; Earl, W.L.; and Merbach, A.E. J. Mag. Res. 29, 11 (1978).

78. van Leeuwen, P.W.N.M.; and Groenveld, W.L. Inorg. Nucl. Chem. Lett. 3, 145 (1967).

79. Bosnich, B.; Poon, P.K.; and Tobe, M.L. Inorg. Chem. 4, 1102 (1965).

80. Anichini, A.; Fabbrizzi, L; and Paoletti, P. Inorg. Chim. Acta 24, L21 (1977).

81. Zeigerson, E.; Ginzburg, G.; Schwartz, N.; Luz, Z.; and Meyerstein, D. J. Chem. Soc. Chem. Comm., 241 (1979).

82. Lo, S.T.D. and Swaddle, T.W. Inorg. Chem. 15, 1881 (1976).

83. McAuley, A.; Macartney, D.H.; and Oswald, T. J. Chem. Soc. Chem. Comm., 274 (1982).

84. Marwedal, B.J.; Kurland, R.J.; Kosman, D.J.; and Ettinger, M.J. Biochem. Biophys. Res. Comm. 63, 773 (1975).

85. Cairns, C.; McFall, S.G.; Nelson, S.M.; and Drew, M.G.B. J. Chem. Soc. Dalton, 446 (1979).

86. Rakowski, M.C.; Rycheck, M.; and Busch, D.H. Inorg. Chem. 14, 1194 (1975).

87. Lancaster, J.R. Jr. Science 216, 1324 (1982).